A Stochastic Model for the Power Situation Indicator: An Extreme Value Theory Approach

by

Junhua Zhong

MASTER THESIS

Master of Environmental and Development Economics

(Master of Philosophy)

Aug 2009

Department of Economics
University of Oslo

Preface

I thank my supervisor at the Department of Economics, Professor Tore Schweder, whose enthusiasm and support, constructive feedback and generosity in sharing ideas and thoughts have been great motivation factors throughout the writing process.

I am also very thankful for my parents and sister. You shape my mind. Without your guidance and support, I would have never arrived at this stage.

Finally but not the last, I thank Professor Olav Bjerkholt, whose instructions lead me to a higher level in academics.

Of course, I am responsible for any possible mistakes or flaws in this thesis, completely.

Junhua Zhong

Oslo, Aug 2009

Contents

List of Figures

List of Tables

Abbreviations

Expression	stands for
CDF	Cumulative Distribution Function
EVT	Extreme value theory
gencos	generation companies
GEV	Generalized Extreme Value Distribution
GPM	Generalized Pareto model
GWh	Gigawatt Hour
IID	Independent identical distribution
MWh	Megawatt Hour
nllh	negative log likelihood
NVE	Norges vassdrags og energidirektorat (www.nve.no)
PP	Probability Plot
QQ	Residual Quantile Plot
rvs	random variables
SSB	Statistics Norway (www.ssb.no)

Notation	stands for (in the order of introduction)
r_t	Water reservoir level at time t
I_t	Water inflow to the reservoir at time t
g_t	Generation of electricity at time t
s_t	Snow precipitation at time t
V_t	Expected future surplus
$P(g)$	Electricity price as the function of generation g
$\overline{r}$	Reservation level of water reservoir
$\overline{k}$	Maximum installed capacity
λ	Lagrangian coefficients in maximization problems
ρ_t	Rho-ratio at time t
d_t	Demand for electricity at time t
$N_n(\cdot)$	Point process of exceedance
$I_{\{X_i>u\}}$	Indicator variable with $X_i > u$
σ	Scale parameter for generalized extreme value distributions
ξ	Shape parameter for generalized extreme value distributions
μ	Location parameter for generalized extreme value distributions
$u(t)$	Process of threshold
$h(\cdot)$	Inverse-link function
$X_{i,n}$	i^{th} element of an ordered sample which consists of n elements
$F^{-1}(\cdot)$	Inverse of CDF $F(\cdot)$
m	m-year return level

Abstract

In this thesis, a new indicator is proposed to characterize the power situation in deregulated electricity markets. A univariate extreme value model for this indicator is presented to investigate the extreme events in Norwegian power market. The demand and supply side of the power market are considered jointly.

The simulation result indicates that the extreme events in the form of a price strike in 2002/3 could have a return period shorter than 10 years. Based on this result, the reliability of power supply is of some concern. Some regulatory measures would be needed to rectify this potential problem.

1 Introduction

1.1 Background

Before 1990, power markets around the world were vertically integrated and heavily regulated in most countries. This country-specific strategy often comprised local self-sufficiency and limited transmission capacities between countries. In that era, the *energy security* problem was mainly an engineering issue. Utilities are required to maintain a target reserve margin to ensure a desired level of reliability and resource adequacy. By doing so, regulators ensured that integrated utilities could serve the retail load and meet prevailing reliability standards at just and reasonable prices (Adib et al, 2008).

Ever since the inception of electric industry regulation, the reliability of electric service has been a priority of the regulators (Adib et al, 2008). With the introduction of market forces to determine the mix and quantity of resources to serve the end-customers, the reliability issue has more rich meaning than before. It requires not only to fulfill the bilateral contracts between retailers and end customers, but also to serve at a reasonable prices.

In deregulated and relatively closed and hydro dominated markets, the fluctuation in spot prices mirrors the variation in either demand or supply. An extraordinar-

ily low inflow often brings about volatile prices since the changes in production must fully absorb the inflow fluctuations.

So far, historic experience offers limited insights on the reaction to such stresses in deregulated electricity markets (Bye et al, 2008). The latest example is the Californian market breakdown in 2000/01, when low inflow to the hydro reservoirs occurred. In Norway, a recorded extremely low inflow happened in the winter of 2002/03 and summer of 2006. Very limited inflow to the reservoirs during the autumn that year created a worrying supply situation. In December it was considered a danger that Norwegian hydro reservoirs would be insufficient to cover the demand until snow melt in the spring, even combined with heavy imports. The shortage in the supply side pushed the market prices to a high level over 2 times of the normal price in the winter of 2002/03. However, interestingly, the annual drop in inflow in that year compared to normal was only some 6%. It is largely a timing problem about mismatch between the generation capacity and the consumption. As pointed out in Amundsen and Bergman (2007):

> The year 2002 started out quite well with water reservoir levels well above normal in July 2002. Then, very special hydrological conditions appeared during the autumn and winter season of 2002-2003 with a sharp decline of precipitation and water inflow. This was a truly *rare event* likely to recur only every 100-200 years. The result of this supply shock was sharply increasing spot prices at the turn of the year 2002-2003. This is reflected in the increased system and area prices during the annual average of 2003...

A power situation of this kind (adjusted by the price mechanics) is interpreted in my thesis as an *extreme event*. It usually corresponds with extraordinarily high prices due to the limited transmission constraints and marginal production costs. Concerns regarding the robustness of the deregulated power markets rest on whether the mechanisms in the recently deregulated market can ensure sufficient power supply and how frequently would the extreme power situations happen under the prevailing market structure.

In this thesis, the case of Norway is subject to the statistical analysis. Norway is a pioneer country in electricity market deregulation. Upon electricity market liberalization in 1992, competition and abundant electricity generation resulted in lower electricity prices, and generation investments dropped to a minor level. In a year with normal precipitation, hydro power generation is around 120 TWh (as for 2007), corresponding to approximately 99 % of Norway's total power production. Even though Norway is also one of the major petroleum exporting countries, hydropower is still the dominating form of energy. That makes Norway a unique country in the energy mix. However, as electricity consumption continued to grow by 1.5-2 % per year, the Norwegian supply situation has gradually been worsened. A comfortable generation capacity margin has disappeared, and the energy balance in an average hydrological year has turned from surplus to deficit balance (Glende et al, 2005).

Due to the large share of hydro capacity in the Nordic market, inflow variation severely impacts power prices. For this reason, the uncertain power situation is more of a concern for the energy security in Norway than other Nordic countries. Demand for power is highly *weather-sensitive* within some intervals. On the other hand, supply varies mainly due to the hydro power which is directly related to the precipitation in two different areas[1]. The precipitation contributes a lot to the variation of generation capacity. For instance, an unprecedented decline of precipitation can bring about supply shock, which in the normal case pushes up the price. And inflow uncertainty and price uncertainty are of particular importance for explaining varying financial performances for the gencos.

Being aware of this uncertainty in the physical side of the electricity, some doubted whether liberalized electricity markets could be expected to produce adequate levels on a continuous basis and at reasonable prices (Vries and Hakvoort, 2004). However, some economists asserted that the deregulated markets can handle the abrupt shortage in inflows well (Bye et al, 2008). But so far in the literature, hardly anyone has analyzed the power situation in Norway and its eco-

[1]They are southern Norway Elspot area (NO1) and central/northern Norway Elspot area (NO2) as defined by Statnett.

nomic implication from a quantitative perspective, and hence failed to capture the essence of what is really happening in practice. To rectify the shortcomings in the prevailing methodology, this thesis establishes a quantitative model to investigate: *whether leaving the power markets to adjust themselves to ensure the energy security is a prudent choice.*

1.2 Research Objectives

Johnsen et al (2001) pointed out that empirical electricity market studies in general and in particular studies with a simultaneous treatment of demand and supply are rare. In many statistical models, lots of effort has been taken in the modeling of power demand or inflow. Hardly anyone combines both demand and supply, with emphasis on uncertainties and random variation. In this thesis, a new measurement addressed as the *rho-ratio* with *simultaneous treatment* of demand and supply is proposed to describe the power situation. Different from the ratio adopted by Visudhiphan and Ilic (2000), the ratio is an ex post concept. The idea will be technically described in section 4.

This simultaneous treatment is especially important in the hydro-based Norwegian electricity sector. By utilizing the time series data of Norwegian power demand and production, I am going to find out the statistical implication of the reliability in power production. I will investigate the extreme behavior of this rho-ratio based on the historical data in relatively short run. A numerical model by using extreme value theory (EVT) gives the distribution of extreme rho-ratio and its return level over different horizons. It helps to answer the question: how likely is it for an extremely severe power situation to occur where prices reach high levels in the short run. I also consider the long run case under more restrictive assumptions.[2]

The conclustion of my analysis is expected to give some policy implications for regulators. Reliability of electric service has been a priority of the regulators

[2]The resulting model may not be directed toward long-term forecasting of the demand/supply ratio, since we don't take into account the intrinsic growth of demand and scheduling capacity built-ups, nor does we account for climatic changes that are under way.

since the inception of electric industry regulation. In the presence of rapidly changing technology and increasing opportunities for choosing wholesale suppliers, regulated utilities are in a process toward unbundlement(Adib et al, 2008). Regulators need to address the maintenance of a prudent reserve margin that meets the reliability needs of newly restructured markets while avoiding imposition of unnecessary expenses on customers. The model in this thesis, in my view, helps to better understand the reality in a deregulated electricity market mainly based on renewable power production utilities such as water falls, wind or ocean waves. The case I select is Norway since 2001 where hydro power is completely dominating as mentioned above. The same analysis may easily apply to other countries, the energy profile of which maybe more complicated.

This thesis is organized as follows: Next section presents the physical side of hydro power production and electricity demand. Section 3 discusses the gencos' decision problem and the probable measures of government's intervention. Section 4 formulates the new indicator addressed as rho-ratio and discuss the underlying reasons. Section 5 provides the data profile(5.1) and the point process model is constructed in (5.2). Section (5.3) gives the diagnostics of the model. Return level estimation is in section (5.4). Section 6 concludes and gives remarks on future potential research in this field. The Appendix gives my computer programs in the statistical language **R** [3].

[3]R version 2.7.2 (2008-08-25); Copyright (C) 2008 The R Foundation for Statistical Computing; ISBN 3-900051-07-0

2 Uncertainty and random variation: the physical side of the hydro power

Hydrological issues and characteristics of hydro power production systems set up both the production possibilities and constraints for the hydro power scheduling problem.

As we are going to find out in the following subsections, the source of uncertainty mainly consists of the variation in inflows to the reservoirs and the stochastic prices. How the spot price is determined in deregulated electricity markets is quite different from what it was before restructuring. For instance, in Nord Pool, the spot price is set day ahead for each hour. And it can be traded constantly across Nordic countries. Supply and demand, both of which determine the spot price, vary due to a range of factors. These factors include e.g. temperature, precipitation, wind conditions and availability of production capacity. The following sections discuss the demand and supply side separately.

2.1 Spot price discovery

The spot price, given as the intersection between demand and supply, is not very sensitive to demand shifts when the demand is low, since the supply stack is typically flat in the low-demand region. However, when demand is high and current generation capacity cannot backup the demand sufficiently, even small increments in demand can have huge effects on the price.

The supply stack is the ranking of all generation units of a given utility or of a set of utilities in a given region. This ranking is based on many factors, such as the marginal cost of production and the response time. The utility will typically first dispatch nuclear and hydro units (in Norway, hydro is the first choice), if available. Hydro power is followed by coal units, oil and gas units in order. The market clearing price is determined by the relative position of demand and supply curves.

The Nord Pool area would be a combined market if there were no transmission

constraints. In an ideal market with greatest efficiency, the electricity is traded at a universal price. This price is called the system price. Nevertheless, local deviations from system price prevail due to the limited transmission capacity. If the transmission capacities are binding at the system price, area prices develops. For areas with ample supply, the area price will be lower than system price, and vise versa.

An important empirical observation is that prices are usually lower in summer than winter, although unexpected shortages such as in 2006 can drive up summer prices. In a hydro-dominated market, the unexpected inflow, snow and temperature conditions explain a large part of the variation in the electricity generation, demand and price.

A local, competitive hydro power market with storage will realize a market price equal to the expected future power price. This result is depicted in section 3. Trade opportunities with neighboring areas will be used to reduce the implications of uncertain water inflow in the future. The storage in the local area will be used to make expected future trade low. With optimal storage, lower or higher than expected inflows in the future are compensated for by import or export and the probabilities of becoming import constrained or export constrained are equal.

If the current reservoir level is high, the agents face more substantial constraints from predetermined reservoir content. The opportunity cost is high. On the opposite, if the current reservoir level is low, it is more likely for the agents to hold the capacity by storing the water until the price is sufficiently high. Of course, they should also take into account the forecasted inflow and spot price in the future. Good timing is essential.

We can summarize the process of spot price determination with following diagram:

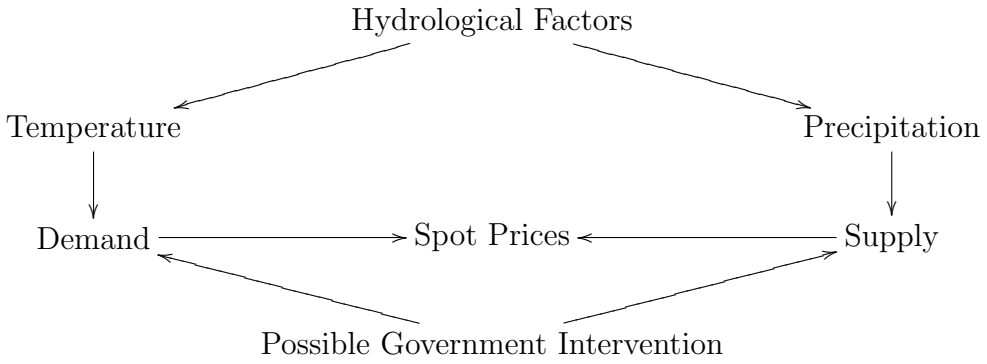

2.2 Demand for the electricity

Demand for electricity can be roughly divided into three parts, industrial demand, residential demand and transmission losses. The main factors affecting electricity demand in short-term are seasonal variation and weather conditions.

2.2.1 Seasonal patterns

Demand exhibits seasonal fluctuations, in yearly, weekly and daily patterns. In Norway the demand-peak normally takes place in the winter due to the excessive heating demand. Unexpected conditions can bring about sudden and dramatic shocks to the demand. For instance, during national holidays or strikes, industrial activities terminate, and the demand drops significantly.

It is widely accepted that, even though regulatory entities are taking their efforts to introduce demand participation into the current retail markets, the demand can still be assumed to be inelastic to the spot price. To improve customers' exposure to price signals is cherished in a wide variety of programs. Some electricity-intensive industry may adjust their production in the case of high prices. But hardly any program allows for fully participation of consumers in price risk sharing. (Households may not respond to the high spike price by turning off their stoves or drop cooking[4]. For market-based demand, it's unrealistic to shift between several production procedures to avoid the high price hours.) Assuming

[4]In many countries, the electricity used for cooling is a major part of the total electricity consumption, but it's not the case in Norway.

inelastic electricity demand is therefore realistic, and it also facilitates my analysis.

2.2.2 Weather-sensitive demand

This part is the most unpredictable in scheduling. Since the warming devices mainly use the electricity, the out door temperature has a substantial effect on demand in all the Nordic countries except Denmark (Laukkanen 2004). The weather-sensitive models are convincing in projection for the demand. The popular treatment is to split the total demand into three parts: fixed industrial part, temperature dependent component and a noise term. Within a certain interval, the demand and temperature is approximately linear. The lower the temperature the higher the demand for electricity, which fits perfectly our empirical observation.

2.3 Supply side of electricity markets

There is a huge difference between electricity markets and other physical markets, that is, the electricity is a commodity which must be generated and consumed simultaneously. The generators have the obligation to provide the electricity that customers need due to the bilateral contracting. On the occasion when the production capacity is not enough to fully cover the demands, the gencos will import from other Nordic areas to fill the gap. The transportation between areas is subject to the transmission constraints, and also induces some cost in energy loss.

One of the advantages of the hydro power is the *storability*. Storability varies in extent among different forms of power. Some forms of power, for example wind power, are difficult to store and control. While, hydro resource is storable in the water reservoir. The withdrawal of water is subject to the decision making of producers. The gencos can smooth the production across periods through reservoirs. Other forms of energy, for example the wind power, can also be stored by pumping water into the reservoir. The potential of storing water which often implies that the gencos have the possibility of varying production over periods, so that they could take the advantage of price variation. Their generation activities

are price-dependent.

But at the same time, they have to face the high opportunity cost of producing today. The stochastic inflow gives high volatility in prices over seasons and between years. The opportunity cost depends on the expectation and variance of water inflow. The uncertainty then affects the production decision at any time.

Seasonal patterns are obvious in the production of electricity. Since electricity consumption is greatest in winter, a good deal of the precipitation from early summer to autumn is stored in the reservoir, and then released through the turbines during the winter. Seasonal patterns therefore exist in the hydro power production, instead of a completely stochastic process [5].

Uncertainty mainly stems from the *stochastic inflows* to the reservoirs and the temperature[6]. Inflows play an important role in the determination of generation capacity. In a hydroelectric power system, the supply depends on the water availability, which is determined by storage from the previous week and the current inflow. High rainfall generally results in an increase before the onset of winter. Precipitation during winter is less and usually in the form of snow which only melts next spring. It also varies during the year, depending on local geographical and climatic conditions. In addition, the demand for electricity depends heavily on temperature. Consequently, nature is expected to be a major determinant of the electricity price. An important characteristic of a hydro system is that market prices may vary greatly in a few months, or even weeks, depending on variations in inflow in addition to variations in consumption. This capacity is vulnerable to the fluctuation of weather conditions. An extremely dry winter or cold winter has great influence to the hydro power production. Normally the colder the weather is, the more serious the shortage of generation capacity would

[5]Other forms of power have no similar characteristics. For example, thermal power has no seasonal patterns. One exception is the wind power which varies over the seasons within a year, but its patterns are not as obvious as the hydro power.

[6]Other factors like the reliability of the transmission is out of the scope of this thesis, even though it is part of the risk profile.

be.

As hydro power is a major source of electricity in Norway and Sweden, availability of the water is the biggest factor that affects the production and henceforth the price pattern in the Nordic power market. Production decisions of hydro power producers are driven by water reservoir level and expectations of inflow, market price and consumption. Also competitors' actions must be considered when making production plans. Regulation limits and capacities of water reservoir and turbines set limits for hydro production.

In addition to short term management of water reservoir, there is long term strategic management based on forecasting in precipitation. Some studies predict patterns of *global climate change* in Norway in the long-run perspective (up to 2050), which conclude that warming rates will be higher in winter than in summer, inland than along the coast, and in the north than in the south. And the increase in precipitation is predicted to be significant in all regions of Norway except the south-east. Precipitation is also expected to be more variable (Hanssen-Bauer et al, 2003). By knowing that both temperature and precipitation will increase in Norway, with greater changes in the North, but the rate of increase will vary with space and seasons, we might have a better knowledge related to the energy sufficiency. These issues are closely related to even more hydrological studies and invite further researches.

Before going into the scheduling problems of production, it's necessary to know the dynamics of water reservoir, by which I am going to preprocess the data for weekly inflows to the reservoir. This is because the data on daily or weekly inflow to the reservoir is not available and the data on precipitation is not a good proxy. First of all, the relationship between different quantities needs to be pinned down with an equation called hydro balance.

2.3.1 Hydro balance

Let's consider a three-period case, where the current period is denoted t, $t-1$ for the previous period, and $t+1$ for the next period. Change in the reservoir

level [7] r_{t+1} in period $t+1$ equals to the inflow I_t less the total discharge for hydro-production at time t, g_t, taking into account the physical restrictions of the reservoir. If the reservoir level is too close to the maximum level (which is determined by NVE[8]), then a part of the reservoir must be spilled for security or environmental reasons. This amount is represented by s_t in equation (1). The change of the reservoir level must obey the hydro balance as

$$r_{t+1} = r_t + I_{t+1} - g_t - s_t \tag{1}$$

where r_t stands for water reservoir level in period t. I_t stands for inflow, g_t for generation and s_t for spillage.

The s_t is prevented from occurring by gencos as possible as they could. It represents lost opportunities for power generation. It happens when the production plan coincides with unanticipated precipitation. Due to the safety reasons, spillage in some cases are conducted as a cushion for the unexpected water inflow in the future. However in the reality, it hardly happens especially in winters, when the capacity of accommodating more inflow is always available. Hence it is assumed to be zero throughout my analysis. This assumption is reasonable and is not critical (Vehvilainen and Pyykkonen, 2005).

The predetermined volume of reservoirs along with the institutional and regulatory constraints imposed on them constitute the constraints for capacity. We will use the hydro balance in section 5.1 to calibrate the data for weekly inflows.

3 Scheduling of Production

In a deregulated market, production decisions are left to market forces. Gencos are presumed to manage their water reservoirs to generate the highest possible

[7] In this thesis, the usage of 'reservoir level' is slightly different from 'storage', in a sense that the former refers more often to the physical content and the latter is more of an economic capacity, usually measured in Mwh units.

[8] Present maximum level should not be exceeded is 95% and 15% is the minimum level to maintain.

income from power production. Their decision regarding hydro power scheduling boils down to how to optimally allocate water over time, treating inflow and prices as stochastic variables. The gencos update their information regarding these variables continuously. We can state their objects as:

> Given a forecast of future market price(spot price)[9]; Establish a generation schedule (or strategy) that maximizes expected profit over the planning period, all relevant constraints taken into account. (Fosso et al, 1999)

The timing optionality can be analyzed on the seasonal time resolution or even time block one. But the management of hydro reservoirs used to be based on dynamic programming techniques that do not include market or strategic considerations (Crampesa and Moreauxb, 2001).

3.1 Factors that determine the scheduling

We first look at the factors that affect the production decisions, such as prevailing area prices[10] and expectations for the future prices and inflow, and plans and opportunity cost of storing water for later use. Hydro power generated by withdrawal of reservoirs has strong price-dependency. For instance, gencos will produce more hydro power when the market price is high. When the price drops, some gencos will hold up the capacity into the future until the price rebounds. But it's the prevailing reservoir levels and future inflows that determine gencos' capacity. For these reasons, gencos with hydro power plants are highly interested in current reservoir levels and the future inflow. And the reservoir levels we observed in different periods encompass the *price effect* to the gencos' production scheduling.

[9]The weather forecast is also taken into account in the firms' scheduling of generation, even though there is no clear evidence that the gencos are using some specific models for weather forecasting.

[10]The gencos are assumed to be price takers.

In summary, three factors contribute to the decision making for the generators. They are:

1. Current reservoir level.
2. Forecasted future inflow.
3. Spot price forecast.

The data for current reservoir level is published by NVE every Monday, which is a public information accessible for every market player. The gencos study the reservoir levels to assess the overall supply capacity. The last two elements above is based on the observation as follows: The gencos may have the ability to forecast the electricity price in the long run and make necessary adjustment to the production levels, so that they can take advantage of the supply position. Future inflows can be estimated by market participants' private models. Empirically, on the market level, gencos' decision can only be observed through hourly aggregate production volume and the corresponding price. Their technologies of forecasting and how they are making bids is pushed into the background and not disclosed to the public.

3.2 Gencos' first best decisions on production

In the absence of government intervention, at least it is the case before 2005, gencos' decisions on production are taking the form of stochastic dynamic programming problem. Some theoretical models can help to understand the dynamics of supply capacity. The overall capacity is determined according to the spot price and independent from single genco's decision making. The following equilibrium model (Johnsen, 2001) will explain why the price expectation can be removed from the representative gecon's point of view.

The representative gecon's problem in the current week (t) is to select a water reservoir level that will maximize the flow of expected future surplus (V_t). The surplus is the integral of demand curve in price form ($P(g)$) over the interval of

$[0,\ g_t]$ plus the terminal value of water reservoir. We assume the producers to have a longer horizon when deciding terminal conditions than simply aiming to empty the reservoir in last period. So the terminal value (V^*) depends on the water and snow volumes left at the end of the planning period. [11]

$$V^* = Ar_T + BS_T + C(r_T + \gamma_s S_T)^2 \tag{2}$$

where A, B, C and γ_s are coefficients. S_T stands for snow stock at the period T. $C(r_T + \gamma_s S_T)^2$ represents the quadratic part of the value function. The planning period is assumed to be one year (52 weeks) without regarding the cross-year storage planning. The final week is defined to be the last week before snow melting starts, when the reservoir levels are normally the lowest. [12]

The planner's optimization problem is to maximize the expected surplus from week t to T and terminal value V^*. The costs of storage and production are negligible since we concern the short-term scheduling problem. It's assumed that producers are risk-neutral. The interest rate is zero. There is no spillage during the planning periods.

$$\max_{\{r_t, r_{t-1}, \cdots, r_T\}} E_t \left[\left\{ \sum_{j=t}^{T} \int_0^{r_{j-1}+I_j-r_j} P(g)dg \right\} + V^* \right] \tag{3}$$

This maximization problem is subject to some physical constraints. The first one is hydro-balance explained in section (2.3.1) restated as following

$$r_j = r_{j-1} + I_j - g_j \tag{4}$$

[11] It can be seen from the first order conditions that introducing snow volumes into the terminal condition has no effect to the optimal reservoir level and is rather trivial to our analysis.

[12] Note that when the snow starts melting is uncertain. In year 2001, 2005, 2006 and 2008, it was on week 18, while in year 2002-2004 and 2007, it was on week 17. A hydro-year is approximately defined to be the year from week 16 to week 17 next year, with a length of 52 weeks.

where I_j encompass the rainfall in energy units I_j^W and snow melting in the one-period ahead snow stack $\psi_j S_{j-1}$

$$I_j = I_j^W + \psi_j S_{j-1}$$

ψ_j is the portion of snow stack melt.
There are also institutional upper and lower reservoir constraints given by

$$r_j \leq \bar{r} \tag{5}$$

$$r_j \geq \underline{r} \tag{6}$$

In Norway, the maximum reservoir level $\bar{r}$ should be maintained is defined to be 95% as a cushion for the future unexpected inflow, and the minimum level is 15% for environmental concern. These are institutional constraints. The upper level of production is limited by maximum installed capacity ($\bar{k}$)

$$g_j \leq \bar{k} \tag{7}$$

This dynamic programming problem can be solved by backward induction. The storage r_T is determined by differentiating the following

$$\begin{aligned} V_T = \int_0^{r_{T-1}+I_T-r_T} & P(g)dg + Ar_T + B \cdot S_T + C(r_T + \gamma_s S_T)^2 \\ & -\lambda_T^U(r_T - \bar{r}) - \lambda_T^L(\underline{r} - r_T) - \lambda_T^g(r_{T-1} + I_T - r_T - \bar{k}) \end{aligned} \tag{8}$$

with respect to r_T. The λ^U , λ^L and λ^g are shadow prices of physical constraints. We hereby get the first order condition

$$-P(r_{T-1} + I_T - r_T) + A + 2C(r_T + \gamma_s S_T) - \lambda_T^U + \lambda_T^L + \lambda_T^g = 0 \tag{9}$$

To simplify the analysis here, we assume the constraints (5) (6) and (9) not binding. Thus the first order condition above can be further reduced to

$$P_T = A + 2C(r_T + \gamma_s S_T) \tag{10}$$

Rearranging the above equation yields

$$r_T = \frac{1}{2C} P_T - \gamma_s S_T - \frac{A}{2C} \tag{11}$$

which is the terminal condition for the reservoir.
Next, we move one week backward to $T-1$. To maximize

$$V_{T-1} = \sum_{j=T-1}^{T} E_{T-1} \int_0^{r_{j-1}+I_j-r_j} P(g)dg + E_{T-1}V^* - \lambda_{T-1}^U(r_{T-1} - \bar{r}) \\ -\lambda_{T-1}^L(\underline{r} - r_{T-1}) - \lambda_{T-1}^g(r_{T-2} + I_{T-1} - r_{T-1} - \bar{k}) \tag{12}$$

we differentiate the above equation with respect to r_{T-1}[13]. The f.o.c is

$$P(r_{T-2} + I_{T-1} - r_{T-1}) = E_{T-1}\left[P(r_{T-1} + I_T - r_T)\right] - \lambda_{T-1}^U + \lambda_{T-1}^L + \lambda_{T-1}^g \tag{14}$$

By combining (11) and (14), we can solve the r_{T-1} as a function of I_{T-1}. The general condition for week j is

$$P(r_{j-1} + I_j - r_j) = E_j\left[P(r_j + I_{j+1} - r_{j+1})\right] - \lambda_j^U + \lambda_j^L + \lambda_j^g \tag{15}$$

If we further assume the constraints are not binding (this assumption is given in equation (7)), the general condition above can be reduced into

[13]To see this, we can write equation (13) into

$$V_{T-1} = \int_0^{r_{T-2}+I_{T-1}-r_{T-1}} P(g)dg + E_{T-1}\int_0^{r_{T-1}+I_T-r_T} P(g)dg + E_{T-1}V^* - \lambda_{T-1}^U(r_{T-1} - \bar{r}) \\ -\lambda_{T-1}^L(\underline{r} - r_{T-1}) - \lambda_{T-1}^g(r_{T-2} + I_{T-1} - r_{T-1} - \bar{k}) \tag{13}$$

$$P_t = E_t(P_{t+1}) = E_t(P_{t+2}) = \cdots = E_t(P_T) \tag{16}$$

Equation (16) is a principle governing the arbitrage activities of individual gencos for the competitive power market setting. Speculation will drive the current price to such a level where no expected net gain from storage can be expected. It also implies that no arbitrage from holding the capacity into the future periods for the power market as a whole. This result is not counter-intuitive, since one genco's storage activities driving up the current electricity price make it more attractive for other gencos to produce more in current period. As a result, the smoothing effect in the long term is not expected from the perspective of the social planner. The supply side as a whole is then more vulnerable to the shock from stochastic inflow and demand than individual gencos' arbitrage behavior.

My analysis justifies the empirical observation in the winter of 2002/03. In that year, the total inflow is only 6% less than the mean value, while the price adjustments were substantial. The problem is that the shortage of inflow in winter cannot be alleviated by holding the ample water in summer over months due to the lack of motivation and limited capability of forecasting.

This finding justifies that we can peel off the arbitrage activities of some agents, i.e. the market power effects in the analysis of power situation. In a market where agents can have the opportunity to exercise their market power, overall output still depends heavily on prices, not the capacity holding of some agents. When a firm does exercise market power, all firms in the market benefit. In fact other firms may benefit more than the company that is exercising market power. This is because the company that is exercising market power reduces its sales, or risks doing so, in order to raise the market price. Other firms do not have to reduce their output in fact they may even increase output but still benefit from receiving the higher market price. Thus, even a small price-taking firm in a market is likely to have a strong incentive to resist attempts to detect or undermine the exercise of market power by other firms (Borenstein, 2000).

According to this model, from the perspective of social planners, it is the best choice to leave the functionality of electricity pricing to the hands of the market. Before 2002/03, Norwegian government actually followed this market rule. As it is going to be shown in the next sections, the availability of capacity *cannot* be ensured by this rule. In fact, after the extreme events in the winter of 2002/03, the Norwegian government published a White Paper[14], extending the responsiblity of *Statnett* as the system operator. *Statnett* should evaluate and develop measures in order to secure the real time balance during the entire winter season. The objective is to avoid rationing in dry years as far as reasonably possible. However, new measures to be applied must not affect the electricity market to any extent. The next sections are going to answer why these measures are necessary.

[14] *Om forsyningssikkerheten for stroom mv.* published by Ministry of Petroleum and Energy, St.meld.nr. 18 (2003-2004).

4 The rho-ratio

An indicator characterizing the power situation from the social planner's point of view is proposed in this section.

4.1 Assumptions

The following assumptions hold throughout the models in this thesis.

1. Climate is stochastic but stationary with a seasonal pattern in the planning period. That means there is no systematic changes in climate in the short run. The relevant processes may have a trending pattern but there is no jump in mean.

2. There is no spillage of water, in effect assuming that in the second period firms supply whatever output can be produced from available water. We have studied the feasibility of this assumption in section 2.3.1.

4.2 The log-rho ratio

In deregulated electricity markets, most producers have committed to meeting demand through contracts with their customers. Such obligations are similar to financial liabilities. The *power situation* is actually a combination of total production and available obligation (in the form of sales commitments) to sell. As an example, having too little power ("'assets"') available for the coming winter represents a risk of demand ("'liabilities"') shortfall.

The question is: how to quantify this market power situation? Visudhiphan and Ilic (2000) proposed a forecasted load and total available supply ratio (demand-supply ratio) as an alternative market concentration measure. I will call this the log-rho ratio, and I will specify this in my context of the electricity market. As an ad hoc screening device, this ratio is used to indicate the likelihood of market power abuse. There are still some shortcomings about this ratio. But in the

case of characterizing a power situation it's still a nice choice. They propose the demand/supply ratio as an index for the market power in mature deregulated electricity markets, acknowledging the fact that the market power will depend not just on market concentration, but also on how demand varies relative to the degrees of excess capacity.

This course of reasoning is adopted to engineer the rho-ratio in my model. This ratio is an analogous to the reserve margin in the analysis of reliability of electric service[15]. It can be written in a form of quotient:

$$\rho_t \equiv \frac{d_t}{r_{t-1} + I_t} \tag{17}$$

d_t refers to the current demand. r_{t-1} refers to the reservoir at the beginning of period (t) and I_t is the inflow realized in period (t). The inflow uncertainty and price uncertainty are of particular importance for explaining varying financial performances for the producers. In Norway, the industry is based on a mix of thermal power and hydro power, with the hydro power dependence making spot prices correlated with the amount of inflow to reservoirs. That is how the inflow data coming in. (Fleten et al, 1997)

This quotient is actually the reciprocal of capacity divided by the demand. A high rho-ratio means the supply available has less potential to backup the demand and vis versa. The higher the ρ_t, the less sufficient capacity to cover the demand, and the more severe the power situation is and vise versa. Based on the analysis to the production scheduling of individual gencos, we define the generation capacity as the sum of reservoir level in previous period and the inflow of current period, which is the denominator of the above equation. This capacity process fully encompasses the information about the gencos' individual choices. Consequently, the price effect has been removed from rho-ratio thereafter.

[15]Reserve margin is one of the measures used in electricity industry to determine the percent of additional capacity above expected demand, which is defined as $\frac{capacity}{expected\ demand} - 1$. (Adib et al, 2008, page 329)

The reason why we take into account the demand and supply simultaneously is also due to the knowledge about the hydrological correlation between temperature and precipitation. Previous study indicates that in those drier winters, the temperature is normally lower, and wet winters are typically warmer, than normal. That means in a technical sense, high demand and low supply capacity are more likely to take place simultaneously. So, the probability of both dry and cold winters is our concern. The most important stochastic climate factors, hydro-inflow and temperature must be handled by taking into account their correlation structure (Vehvilainen and Pyykkonen, 2005).

For the convenience of numerical analysis, we use log-rho instead

$$\rho_t \equiv \log d_t - \log (r_{t-1} + I_t) \tag{18}$$

5 Point process threshold model

Having set up the indicator for power situation, we can proceed to investigate the tail behavior of this indicator. We have actually prepared for the univariate model, since we have turned bivariate point process into the univariate one by formulating the rho-ratio, which greatly simplifies our analysis. By examining the extreme behavior of this ratio, questions like the following can be answered: how probable it is going to be for the gencos to face a severe power situation as in 2002/03. And if there is a quantity characterizing the return level, what is confidence interval? Shall we believe in the numerical predictions?

We first plot the observed rho-ratio to see if it reflects the notable extraordinary power situations in the past 7 years. Then a point process threshold model will be given, by which we can make inferences and simulation (See section 5.2) to answer the question above. Before building up the model and doing statistical analysis, we should examine the data set.

5.1 Data profile

The daily demand data set considered in this thesis was published by NordPool's website. The dataset for water reservoir levels in the 3 areas in Norway is published by SSB (1998-2004) and NVE (2005 till now) via their websites. The publishment of the reservoir levels is a compulsory to the Norwegian government.

Under technically efficient production, there exists a one-to-one physical relationship between water and energy. In other words, given the reservoir levels, we could estimate with satisfactory precision the amount of energy that could be produced. This part is done by engineers. The water reservoir levels available are therefore measured by MWh or GWh instead of cubic meters or the like. So the weekly demand and weekly inflow can agree with each other on the unit. This justifies the formulation of the rho-ratio again.

5.1.1 Demand for electricity

The demand data is on a daily basis, which is different from the inflows and reservoir content. To match the frequencies between these two sets of data. It's necessary to add up the daily demand into weekly data. But we can still plot the daily demand to give a better graphical description. Figure 1 plots the series of daily demand form week 9, 2001 to week 26, 2008. In 2001, all 4 countries (Norway, Sweden, Finland and Danmark) had been integrated in a common Nordic market with no cross-border tariffs. (Unfortunately, there is no correspondent *daily* data for the reservoir levels to match such a long series.)

From the graph, we can see the slight climbing pattern of demand from around 2002 to 2008, if at all. Whether this trending is supported by the data is analyzed in Table 1 of Section 5.2.3. The linear trend captures the steady growth in aggregate demand, mainly due to the constant physical investments in industrial infrastructure. In addition, we can observe that there is an obvious seasonal pattern on yearly base, which justifies our interpretation in Section (2.2). The amplitudes are surprisingly even, which indicates that the electricity demand is more stable than the precipitation, the main source for the supply shock. The peaks correspond to the cold days when electricity for heating purpose is normally high.

5.1.2 Weekly reservoir levels

The weekly reservoir content which represents the generation capacity in part (the other factor is the inflows to the reservoir) in the past 10 years is illustrated in Figure 2. The reservation (15% of the reservoir capacity) has been subtracted from the process due to the institutional constraint. (Since that section of 15% of reservoir does not represent the production which can actually take place. They are required by the government for environmental purposes.) This is partly because the inflows are more volatile than the temperature, the main determinant of electricity demand.

Seasonal patterns are also apparent in the weekly reservoir but more fluctuating

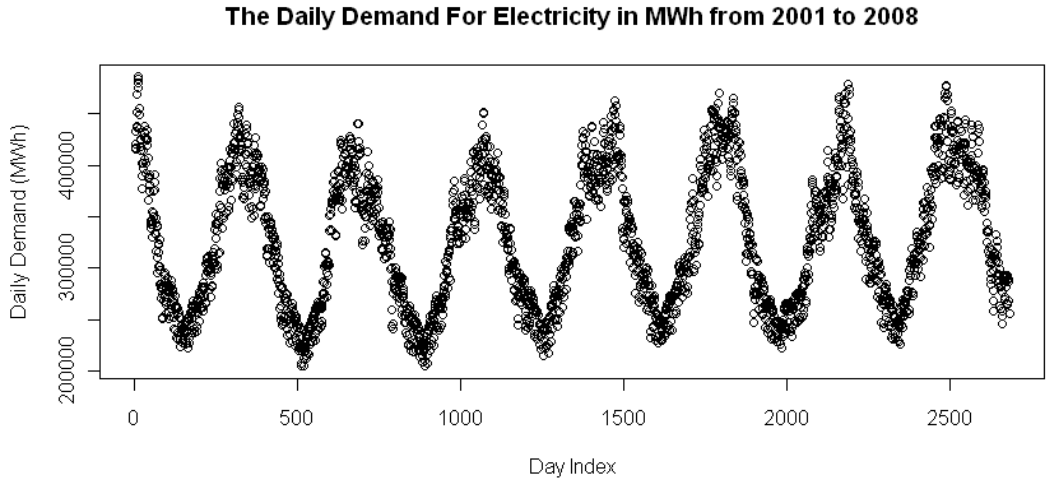

Figure 1: The series of daily demand from week 9, 2001 to week 26, 2008 is plotted. We can see that the data points are more likely to clutter in winters. The numbers at the left upper corner of each block illustrate the year.

because the precipitation is much less stable than the demand brought about by the fluctuating temperature. Compared to Figure 1, weekly reservoir is less regular in pattern and right opposite to the daily demand.

5.1.3 Weekly Inflow Process

From equation (17), we can see that the reservoir level is not all we need. We have to obtain the weekly inflow process (I_t in the denominator of equation (17)). To obtain the series of weekly inflow, we need to invoke the hydro balance in section (2.3.1).

$$r_{t+1} = r_t + I_{t+1} - g_t$$

Having known the weekly reservoir levels r_t and weekly hydro production g_t for 381 weeks, we can calibrate the weekly inflow by rearranging the equation above into

$$I_{t+1} = r_{t+1} - r_t + g_t$$

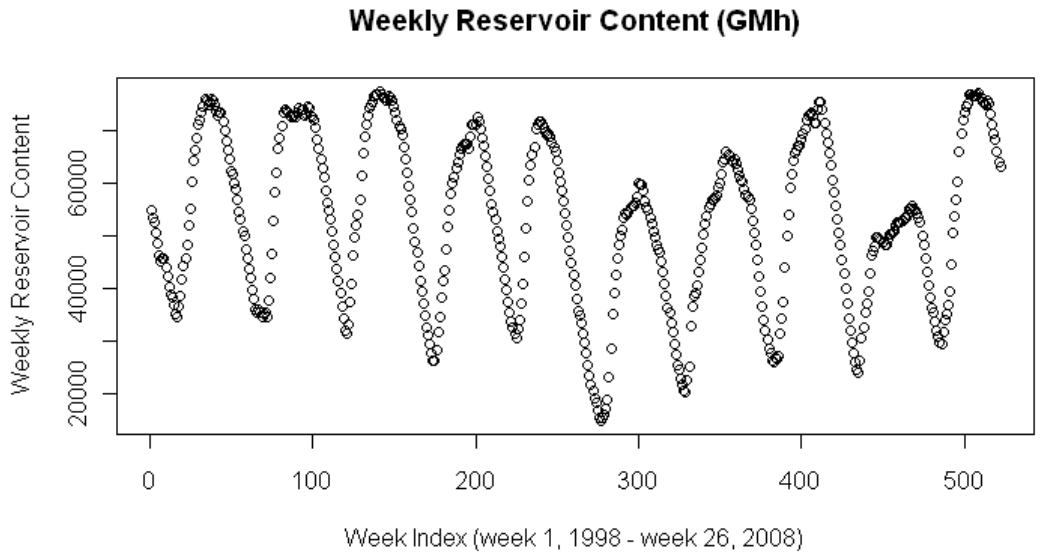

Figure 2: The intervals where points cluster correspond to the late springs and autumns, when the water begins to accumulate in the reservoirs. The intervals where the reservoir levels changes swiftly correspond to the dry winters.

The inflow process derived in this way encompasses the direct inflow and snow-melting water inflow. As the snow melting mechanism does not enter the social planner's model for production capacity allocation in section 3, there is no need to make further distinction between the direct inflow and the snow capacity anymore. Appendix **A** provides the details of **R** procedures to obtain the inflow data.

In Figure 3, the weekly inflow inferred from the reservoir has less obvious seasonal patterns than percipitation. And the non-stationarity is more profound. Note that it is not equivalent to the quantities of precipitation since the series $\{I_t\}$ includes the water inflow caused by snow-melting. (That is the main reason why we cannot use the precipitation as the proxy for weekly inflows in an attempt to rectify the data inefficiency problem.) Intervals where points cluster in general correspond to the dry seasons.

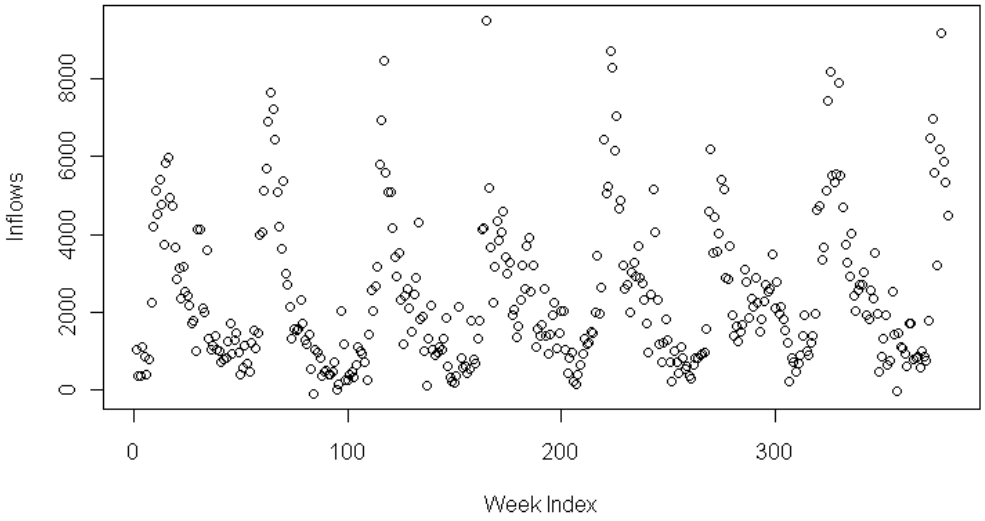

Figure 3: Weekly inflows over 2001-2008. The points where inflow is high in the years are approximately around week 17 or week 18 when the snow melting begins.

5.1.4 rho-ratio

The log-rho ratio, see equation (18), is shown in Figure 4. The rho values in the winter of 2002 and the summer of 2006 are higher than normal level, taking the seasonal patterns into account. What happened in winter 2002 was due to the extraordinary low inflows in autumn, which was analyzed in the introduction.

We can tell from the figure that there is a cluster of points in summer 2006 which are higher than normal years. In week 21 of year 2006, the inflow to Norwegian reservoirs was 4.5 TWh. At this season inflows usually is high, due to snow melt in the mountains. Still the level in week 21 was below normal. Hence, the increase in reservoir levels from week 20 to 21 was below normal. At the end of week 21 the level was 43.0 percent after a 3.4 percentage point increase. In the consequent 12 weeks, this situation persisted until week 32, when the effective inflow in Norway was about half of normal due to low precipitation and drought

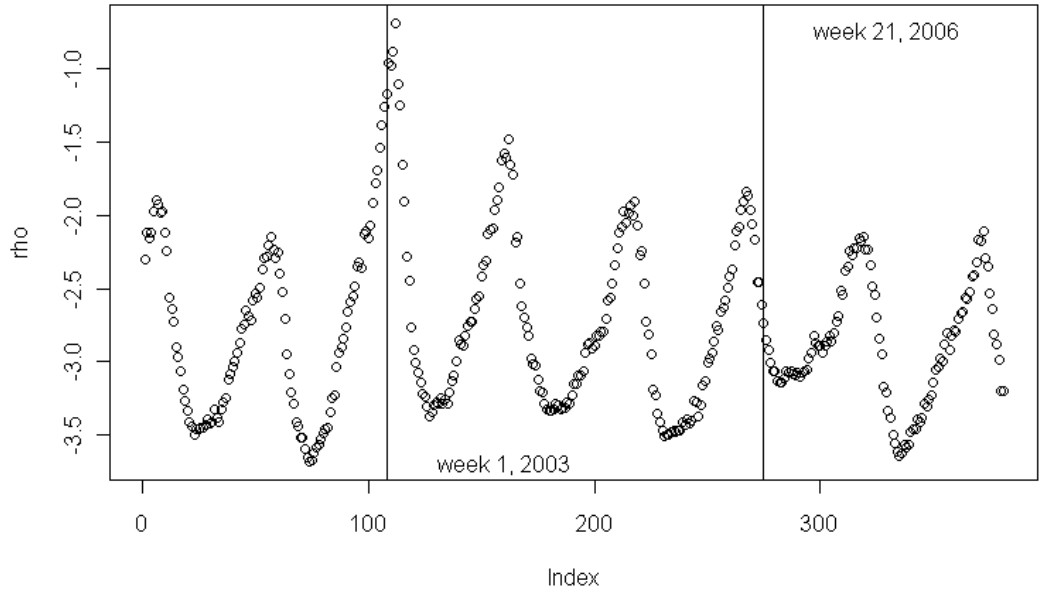

Figure 4: The Log-rho ratio over 2001-2008. From the plotting, we can easily recognize the extreme values in year 2002 and 2006. The vertical lines indicate two different events happened in week 1, 2003 and week 21, 2006 respectively.

in several mountain areas. [16]

5.1.5 Exceedance market power

We need to select a threshold to remove the apparent seasonality in the series of log-rho ratio which should be a time-varying one. Since the parameterization of the point process model is invariant to threshold choice, the only impact of varying a threshold is to affect the bias - variance trade off in the inference (Coles, 2001, page 136). We observe that there is a strong seasonal effect in rho-ratio series and hence select one that accounts for this effect. Nevertheless, the choice of threshold should *not* be arbitrary. It is actually sensible to use a threshold that gives an approximately uniform rate of exceedances throughout hydrological years. The threshold shown below is selected by trial-and-error with this objective in mind.

The choice of u is formulated as

$$u(t) = \alpha_0 + \alpha_1 \cos\left(2\pi t/52.14 + \alpha_2\right) \tag{19}$$

corresponding to a cycle-period of one hydro-year. By trial-and-error, I informally fitted this model to the data shown in Figure 5, resulting in

$$u(t) = -2.6 + .81 \cos\left(2\pi t/52.14 - .18\right) \tag{20}$$

Figure 5 plots the rho-ratio series, augmented with a time-varying threshold. From the plotting, we can easily observe that the unusual values in 2002/03 and 2006, which can be even more obvious in the threshold excesses plotted in Figure 6. We can see the approximately uniform rate of exceedances over hydro-years in Figure 6, where the seasonal pattern is not apparent as in Figure 5.

[16] Details about the power situation of Norway in 2006 can be found on www.nve.no.

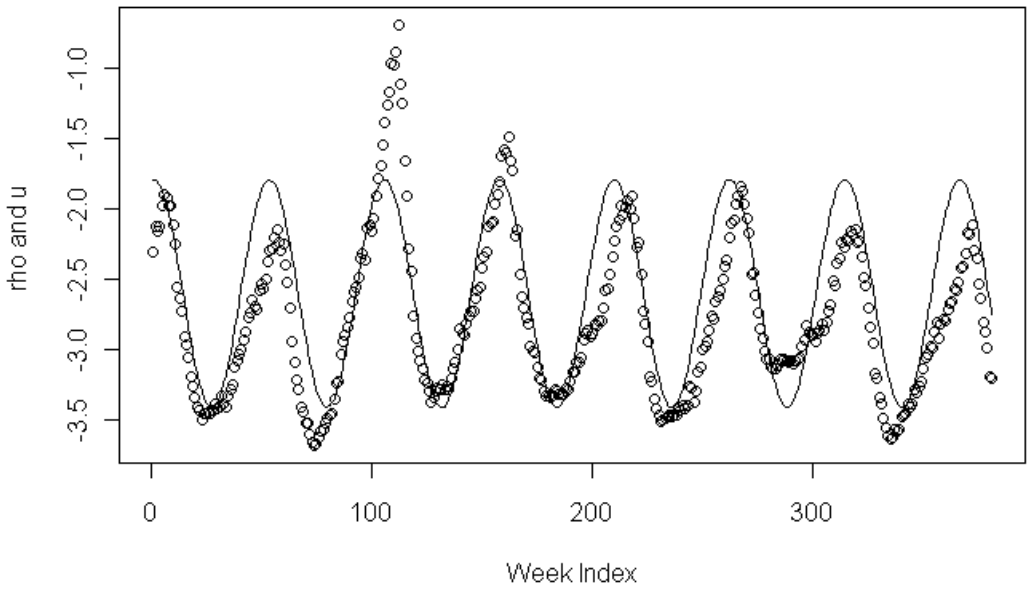

Figure 5: Plotting of the Rho-ratio and time-varying threshold altogether. The solid curve represents the threshold and dots represent the weekly log-rho ratio.

5.2 Point process model

In this section, a point process threshold model is built to analyze the extreme events, for instance, the situation in year 2002/3 and 2006.

Extreme value theory (EVT) is a statistical discipline, providing techniques and models for describing the unusual events rather than usual ones. By definition, extreme values are scarce, the estimation of which often requires levels of a process that are much greater than that has already been observed (Coles, Page vii, 2001). My presentation here is based on Coles (2001).

The point process threshold model is one of the ways which characterize the extreme value behavior of a process. The same process could also be modeled by the generalized Pareto model (GPM) fitting in a sense that it enables a more natural formulation of non-stationary in threshold excesses (Coles 2001, page

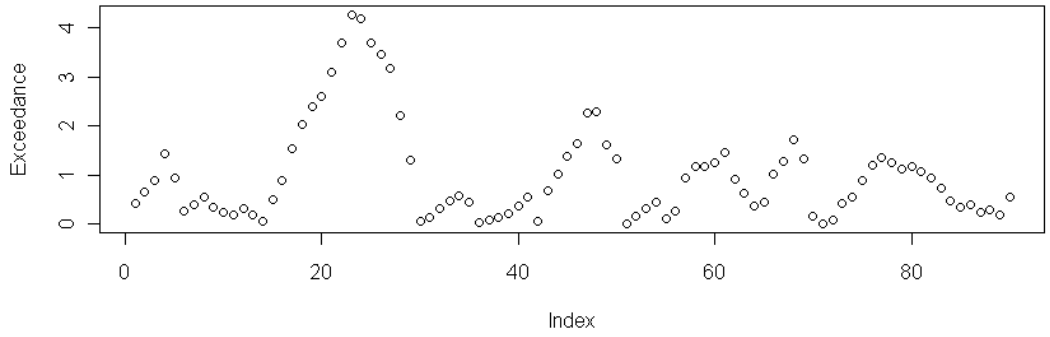

Figure 6: Threshold excess is defined to be $log(\rho) - u$. There are 85 exceedance points in total. The horizontal line indexes the exceedance points in the order when they occur.

124). But I prefer the point process threshold model. It is because that the Point Process model (PP) lets the threshold u be part of the formulation of the likelihood. While in the GPM, the data points X_i that fail to exceed u are simply ignored, namely, they are not incorporated into the likelihood. The embedded information is just out of the model (Coles 2001, page 134). Another advantage of adopting Point process model is that it allows for the treatment of extremes of sequences more general than IID in a straightforward way, which is the classical technique (Embrechts et al, 1997, Page 220).

5.2.1 How the point process is defined

Intuitively, the point process N counts the number of X_i falling into A, which is the subspace of a state space E. It is a random element or a random function which assumes point measures as values. It is closely related to the extreme value theory. As we know the definition of the point process of exceedances can be given as (Embrechts et al, 1997, Page 222).

Definition 1 *Let u be a real number and (X_n) a sequence of rvs. Then the point process of exceedances is*

$$N_n(\cdot) = \sum_{i=1}^{n} \epsilon_{n^{-1}i}(\cdot) I_{X_i > u}, \ n = 1, 2, \cdots,$$

with state space $E = (0, 1]$ *counts the number of exceedances of the threshold* u *by the sequence* $X_1, \cdots, X_n$. *The* ϵ *above is the exceedance rate.*

In the model of section 5.2, $u(t)$ represents the threshold we are going to define. The sequence of *threshold excesses*, which is $EX(t) = X(t) - u(t)$, can be defined as $EX = \{(EX(t), t) : EX(t) > 0\}$. I would like to know the process of threshold excesses for a sequence of increasing thresholds $u = u_n$, which we will choose in such a way that $EX(t)$ converges weakly, to a Poisson random measure. The inferences are based on the asymptotic theory of extreme values, which is in turn built on the weak convergence of point processes. The relevant details are provided in section 5.2.2.

The following explains *why the excesses of a high threshold* u *matter in our model instead of the exceedances by themselves.* Let $X_1, X_2, \cdots$ be a sequence of IID random variables, having marginal distribution function F. It is natural to regard as extreme events those of the X_i that exceed some high threshold u. For large enough n, we have the following probability mass function (Coles, 2001, P74)

$$F^n(z) \approx \exp\left\{-\left[1 + \xi\left(\frac{z-\mu}{\sigma}\right)\right]^{-1/\xi}\right\} \tag{21}$$

for some parameters μ, $\sigma > 0$ and ξ. The log-linearization of the above probability yields

$$\zeta = Pr\{X_i > u\} = 1 - F(u) \approx \frac{1}{n}\left[1 + \xi\left(\frac{z-\mu}{\sigma}\right)\right]^{-1/\xi} \tag{22}$$

for large predetermined threshold u. For a variable X_i that exceeds u, the likelihood contribution is

$$Pr\{X_i = x\} = Pr\{X_i > u\}\, Pr\{X_i = x | X_i > u\} = \zeta \cdot f(x - u) \tag{23}$$

where $f(\cdot)$ denotes the density function of the generalized Pareto distribution. Clearly, it is the threshold excesses ($EX = x - u$) as defined above that enter the calculation of likelihood instead of exceedances x.

5.2.2 Likelihood inference

Let $X_1, \cdots, X_n$ be IID, having marginal distribution function F. With $M_n = \max\{X_1, \cdots, X_n\}$, there are sequences of constants $\{a_n > 0\}$ and $\{b_n\}$ such that

$$Pr\{(M_n - b_n)/a_n \leq z\} \to G(z) \tag{24}$$

with $G(z)$ following a generalized extreme value (GEV) distribution

$$G(z) = \exp\left\{-\left[1 + \xi\left(\frac{z-\mu}{\sigma}\right)\right]^{-1/\xi}\right\} \tag{25}$$

for some scale parameters μ, $\sigma > 0$ and shape parameter ξ. And let z_- and z_+ be the lower and upper bounds for the support of G. Then the sequence of point processes

$$N_n = \{(i/(n+1), (X_i - b_n)/a_n) : i = 1, \cdots, n\} \tag{26}$$

converges as $n \uparrow \infty$ on regions of $(0,1) \times [u, \infty)$, for any threshold $u > z_-$, to a Poisson process, with intensity measure

$$\Lambda(A) = (t_2 - t_1)\left[1 + \xi(\frac{z-\mu}{\sigma})\right]^{-1/\xi}, \ for\ A = [t_1, t_2] \times [z, z_+) \tag{27}$$

Being a Poisson process (Coles 2001, Chapter 7.1, page 134),[17] the likelihood function of a realization of this limiting process is

$$\begin{aligned} L_A(\mu, \sigma, \xi; x_1, \cdots, x_n) &= \exp\{-\Lambda(A)\} \prod_{i=1}^{N(A)} \lambda(t_i, x_i) \\ \propto \exp\left\{-n_y\left[1 + \xi\left(\frac{u-\mu}{\sigma}\right)\right]^{-1/\xi}\right\} &\prod_{i=1}^{N(A)} \sigma^{-1}\left[1 + \xi\left(\frac{x_i - \mu}{\sigma}\right)\right]^{-\frac{1}{\xi}-1} \end{aligned} \tag{28}$$

here n_y denotes the number of years of observation.

[17] This is a basic result in extreme value theory.

The threshold excess model likelihood can be computed, following the logic of equation (28), based on equation (22) and (23).

$$L(\zeta, \tilde{\sigma}, \xi; x_1, \cdots, x_n) = (1-\zeta)^{n-n_u} \prod_{i=1}^{n_u} \zeta \tilde{\sigma}^{-1} \left[1 + \xi \left(\frac{x_i - \mu}{\tilde{\sigma}}\right)\right]^{-\frac{1}{\xi}-1} \tag{29}$$

where n_u is the number of exceedances of u. And notation $\tilde{\sigma} = \sigma + \xi(u - \mu)$. This basicly how the likelihood in our models calculated. The product term in the above represents the probability that n_u exceedances with value $x > u$, $(1-\zeta)^{n-n_u}$ represents the rest which does not exceed u.

In the following numerical model, I am going to estimate the relevant parameters by maximizing the likelihood in Eq(29). We can now move on to the numerical analysis.

5.2.3 Numerical model

Using the threshold given in equation (20), we can fit the log-rho ratio process in 7 different settings for parameters. The estimated parameters are summarized in the following table.

Models	**p**	β_0	β_1	β_2	β_3	β_4	β_5	β_6	**nllh**
1. Time-homogeneous	3	-1.281	0.832	0.200					-123.45
		(0.276)	(0.259)	(0.137)					
2. As 1. but periodic in μ	4	-2.066	0.759	0.268	0.208				-180.77
		(1.99e-06)	(1.99e-06)	(1.99e-06)	(1.99e-06)				
3. As 2. but periodic in $log(\sigma)$	5	-2.098	0.927	-1.632	0.400	-0.009			-183.52
		(0.058)	(0.068)	(0.226)	(0.170)	(0.144)			
4. As 3. but periodic in ξ	6	-2.185	0.928	-2.005	0.934	-0.111	0.376		-185.66
		(0.046)	(0.047)	(0.104)	(0.079)	(0.043)	(0.043)		
5. As 3. plus linear trend in μ	7	-2.08e+00	-9.96e-05	9.10e-01	-1.45e+00	4.16e-01	1.62e-01	9.54e-02	-183.89
		(1.99e-06)	(1.99e-06)	(1.99e-06)	(1.99e-06)	(1.99e-06)	(1.99e-06)	(1.99e-06)	
6. As 3. plus linear trend in μ, $\log(\sigma)$	8								NaN
7. As 3. plus linear trend in μ, $\log(\sigma)$, ξ	8								NaN

Table 1: Number of parameters (p), correspondant standard errors and maximized log likelihood (in the form of negative log likelihood, nllh) for 7 models fitted to seasonally adjusted rho-ratio series. The *nllh* for the Model 6 and 7 are not available because the settings lead to the failure of convergency of maximum likelihood.

If we assume the exceedance of log-rho series to be time-homogeneous, as we can see in the first row, the estimated scale and shape parameters are

$$\widehat{\mu} = -1.281\ (0.276),\ \widehat{\sigma} = 0.832\ (0.259),\ \widehat{\xi} = 0.200\ (0.137) \tag{30}$$

with standard errors given in parentheses. By examining the $nllh$, we can conclude that the time-homogeneous assumption is inferior to the assumption of non-stationarity. It's necessary to comprise periodic effects in the location and scale of extremal behavior. This is what the estimation tells us.

Furthermore, when we consider the series by itself, the non-stationarity in our process is also apparent. The result from homogeneous model, the parameters of which are given in Eq(30), can hardly stand on its own. The reason is that the non-stationarity in environmental data often departs from IID sequences in two respects: short-range dependence and heavy seasonality (Smith 1989).

In our example we first realize that the extreme values may have a tendency to cluster in some particular periods. That is, the occurring of extremes has some seasonality. It can be observed from negated data points in Figure [5] that the extremes more likely take place in winters. This pattern is in part due to the covariance between temperature and precipitation. Meteorological analysis indicates that: a cold winter is normally a dry winter as well. Adverse temperature and precipitation jointly lead to a severe power situation in the winter. Usually, the case will not be serious when they happen separately. Secondly, extreme values often occur in groups, implying that one extremely high rho-ratio is likely to be followed by another. This is also not a counterintuitive observation, since the serious shortage of generation capacity cannot be relieved very quickly in the winter unless the temperature climbs back to the snow melting point. Consequently, the extreme power situation might persist from a few days to several weeks. That justifies the assumption in my model: rho-ratio series have the property of non-stationarity.

Having realized that the clustering induces short-range dependence in the ob-

servations, we would try to take into account the periodity in parameter vector θ. In the inference of the models, we use the *link function* for generalized linear modeling of θ to capture this periodity. There is a unity of structure of

$$\theta(t) = h(X^T\beta) \tag{31}$$

θ here denotes either μ, σ or ξ. $h(\cdot)$ is the *inverse-link* function, mapping the θ to its covariate (Coles 2001, Page 301). X is the model vector and β is the vector of parameters. The link function $h(\cdot)$ for parameter σ is exponential so as to preserve positivity on σ, and it is an identity for shape parameter ξ and μ in our case. For example in Model 4 (as we can see in Figure [9]), there are 6 parameters (from β_0 to β_5)

$$\mu(t) = [1, \cos(2\pi t/52.14 - 0.18)] \begin{bmatrix} \beta_0 \\ \beta_1 \end{bmatrix} \tag{32}$$

$$log(\sigma) = [1, \cos(2\pi t/52.14 - 0.18)] \begin{bmatrix} \beta_2 \\ \beta_3 \end{bmatrix} \tag{33}$$

$$\xi = [1, \cos(2\pi t/52.14 - 0.18)] \begin{bmatrix} \beta_4 \\ \beta_5 \end{bmatrix} \tag{34}$$

If we further add into the models with linear trend, for example in μ, the setting of Eq (32) would be modified into

$$\mu(t) = [1, t, \cos(2\pi t/52.14 - 0.18)] \begin{bmatrix} \beta_0 \\ \beta_6 \\ \beta_1 \end{bmatrix}$$

Then we use the point process fitting function $fpp(\cdot)$ in **R** package *extRemes*. Details for 7 models of different settings and the estimated parameters are given in Table 1. The procedures in **R** and the relevant explanations to the scripts are

provided in Appendix B.

We can see from Table 1 the evidence for periodic effects in all 3 parameters is overwhelming compared to the homogeneous case in Model 1. This result matches our assumption of non-stationarity. The likelihood ratio tests comparing first 4 models give strong support for model 4. When comparing model 4 and 5, we can see no improvement in allowing a linear trend in $log(\sigma)$ or μ. Elaborately, the *nllh* in model 5 is almost equivalent to the one in model 4, and even less. By introducing more linearity into the model actually breaks down the likelihood references, which corresponds to the failure of model 6 and 7. Hence, model 4 is the most convincing among 5 different forms of setting.

5.3 Diagnostics

The accuracy of the fitted model is supported by probability plots and residual diagnostic plots in Figure 7, 8, 9 and 10. These 2 types of diagrams are constructed by transformation of the point process parameter values to the corresponding generalized Pareto parameters. In our age of nearly unlimited computing power this graphical data exploration is significantly important in that they are more informative for our purposes. In addition to looking into the maximum likelihood estimates as given in Table 1, the graphical data analysis is introduced to diagnose our 7 different models.

Our interpretation is built on the following. We define the *ordered* sample of n exceedances as $X_{[1]} \leq X_{[2]} \leq \cdots X_{[k]} \leq \cdots \leq X_{[n]}$. $F(X_{[k]})$ is defined to be the CDF of the fitted distribution. Note that $F_n(X_{[k]}) = (n-k+1)/n$, where F_n stands for the empirical distribution function of $F(\cdot)$. The graph

$$\left\{ \left(F(X_{[k]}),\ \frac{n-k+1}{n+1} \right) : k = 1, \cdots, n \right\}$$

is the *probability plot (PP-plot).* The *residual quantile plot (QQ-plot)* is also provided in my analysis, which is

$$\left\{ \left(X_{[k]},\ F^{-1}\left(\frac{n-k+1}{n+1} \right) \right) : k = 1, \cdots, n \right\}$$

where the $F^{-1}(\cdot)$ is the inverse of CDF $F(\cdot)$. We have some regulations about the pattern of the plots. If the model provides a good fit to the data, the PP-plot would be approximately around the 45^o line and the quantiles in QQ-plot are linearly related to the corresponding quantiles of a model. Linearity in a graph can be easily checked by eye and can be further quantified by means of a correlation coefficient. This tool could therefore be ideally used when trying to answer the classical goodness-of-fit question: does a particular model provide a plausible fit to the empirical distribution?

There are several patterns which can be recognized in the analysis. Because a change of one of the distributions by a linear transformation simply transforms the plot by the same transformation, one may estimate graphically location and scale parameters for a sample of data, on the assumption that the data come from the reference distribution. And some difference in distributional shape may be deduced from the plot. For example if the reference distribution has heavier tails (tends to have more large values) the plot will curve down at the left and/or up at the right.

Now the 7 models' graphics can be analyzed separately. Among them, Model 4 gives the best fit. However, Model 6 and 7's PP cannot be produced due to **R** fails to converge in calculating likelihood. In Model 2, the model and empirical distribution lie roughly along the 45^o line. That means the modeling distribution fits the empirical data in a sense the model has an acceptable quality of the approximation. Compared to the time-homogeneous version, introducing the periodity in scale parameter μ gives a huge improvement in likelihood. That means the severities of power supply have some cycling patterns, which cannot be recognized instantly from the empirical data. However, the QQ-plot in model 2 is not a strictly linear line, but curves up at the right. The model actually does not take too much into account the outliers in the empirical data represented by the vertical axis.

In addition to the periodity in μ, model 3 introduces the periodity to the $log(\sigma)$. This leads to a slight improvement in $nllh$. While the patterns of PP-plot and QQ-plot are very similar to Model 2, Model 3 still has the problem of not able to account for the outliers in the empirical data.

Model 4 is the best fit among all 7 settings. Compared to the Model 3, it has improved a little in the linearity of the QQ-plot. The distance between the empirical data points and the 45^o line is closer. That means Model 4 can fit the empirical data set better in a sense that more outliers in QQ-plot can be explained by the model.

Model 5 introduces the linear trend in the mean μ, which is assumed to be gradually increasing, in addition to the periodic Model 4. This is a natural assumption, especially in a background of global warming. It is possible to have a trending in the expected severities of power situation. However, the $nllh$ in this model is smaller than Model 4. So this assumption is actually not supported by the empirical data.

The PP plots justify our conjecture that there is no clear linear trend in the power situation process. Even the demand may have grown gradually year by year, the correspondent capacities can meet this need. However, the power situation usually goes wild and has more clustering effects in the winter. That can in part explain the periodity in the 3 parameters in our inference space.

5.4 Return level estimation

Having obtained the best model, we can move on to the next stage by imposing the question: how often does the extreme rho-ratio happen given the present market environment? This question can be stated in another way: how much confidence shall we put on the prevailing market structure? If the extreme power situation happens too often, the functioning of the market should be questioned and anxiousness about the reliability of power supply in deregulated markets with

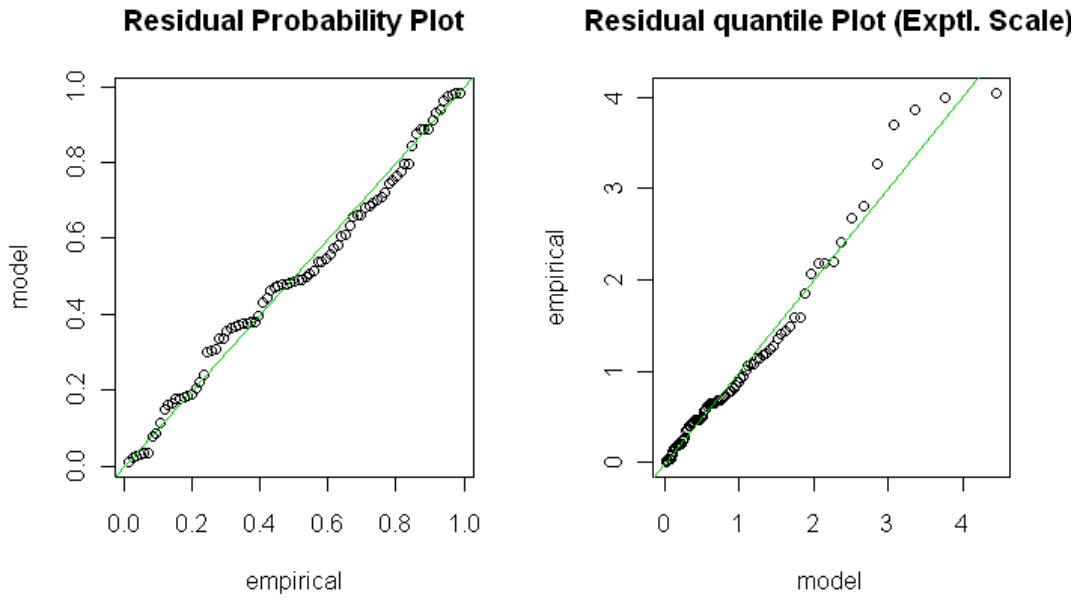

Figure 7: **Model 2.** The model and empirical distribution lie roughly along the 45^o line. Compared to the time-homogeneous version, introducing the periodity in scale parameter μ gives a huge improvement in likelihood.

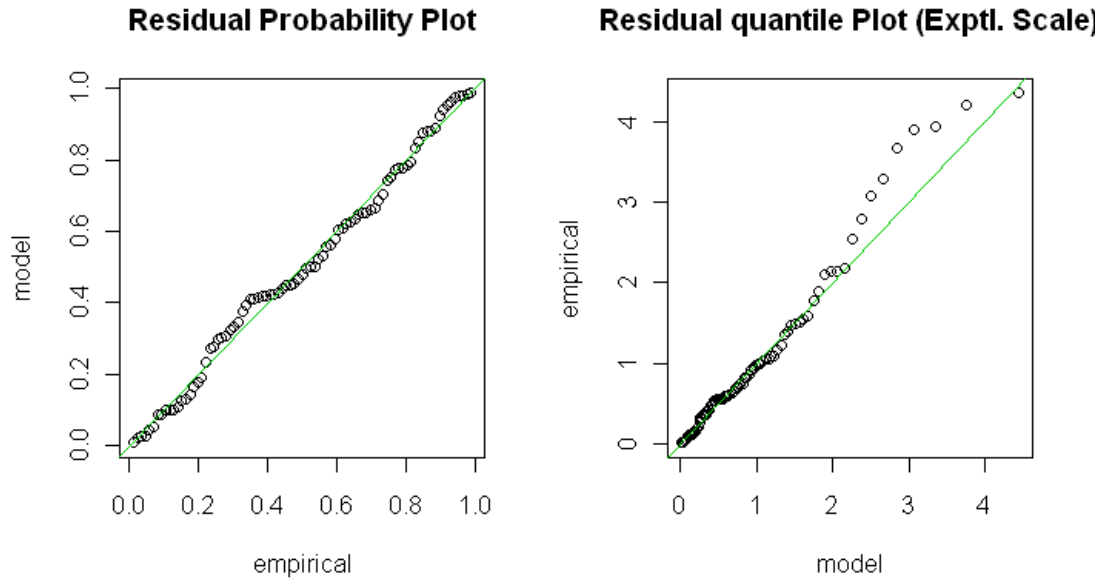

Figure 8: **Model 3.** In addition to the periodity in μ, model 3 introduces the periodity to the $log(\sigma)$. This leads to a slight improvement in $nllh$. While the patterns of PP-plot and QQ-plot are very similar to Model 2, Model 3 still has the problem of not able to account for the outliers in the empirical data.

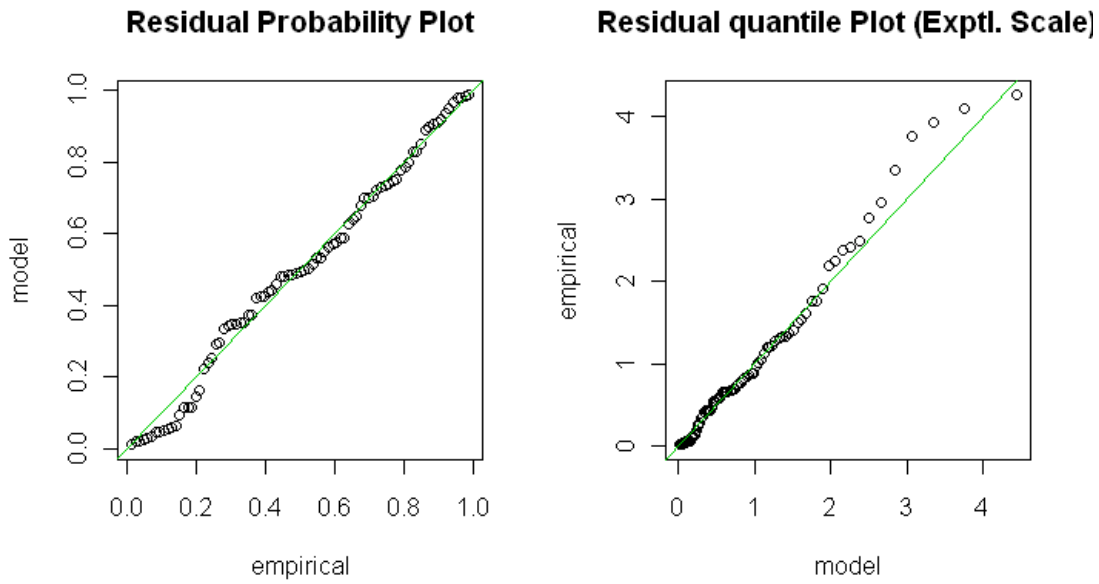

Figure 9: **Model 4:** is the best fit among all 7 settings. Compared to the Model 3, it has improved a little in the linearity of the QQ-plot. The distance between the empirical data points and the 45^o line is closer. That means Model 4 can fit the empirical data set better in a sense that more outliers in QQ-plot can be explained by the model.

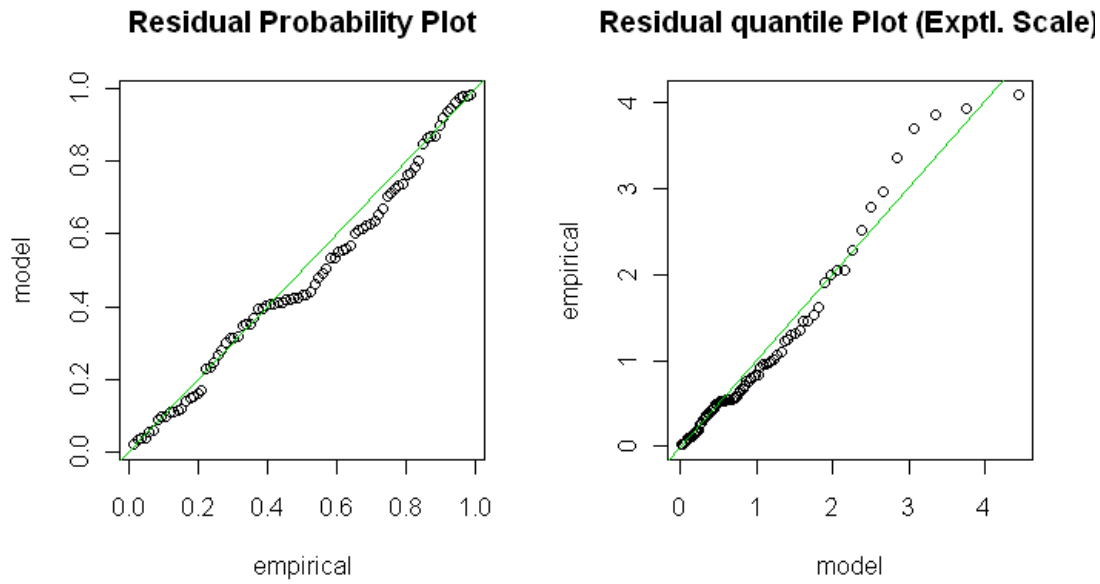

Figure 10: **Model 5:** In addition to the periodic Model 4, this model introduces the linear trend in the mean μ, which is assumed to be gradually increasing. It is possible to have a trending in the expected severities of power situation. However, the *nllh* in this model is smaller than Model 4. So this assumption is actually not supported by the empirical data.

stochastic energy supply cannot be calmed down.

5.4.1 Z_m values based on the chosen model

The model we obtained in the previous section can help to give a numerical evaluation about the return level of some specific lengths of observation. Note that it is an asymptotic result.

Return level estimates can be calculated based on fitted model 4. The precise form depends on the model for nonstationarity (Coles, 2001, page 138). In our case, there is seasonality over a one-year cycle in rho-ratio series. We can't calculate the return level estimates as in the stationary version of the point process model (Remember Model 1 is homogeneous).

By denoting the m-year return level with respect to the rho-ratio as z_m and letting n be the number of observations in a year, z_m should satisfy the equation

$$1 - \frac{1}{m} = Pr\left\{max(X_1, \cdots, X_n) \leq z_m\right\} \approx \prod_{i=1}^{n} p_i \tag{35}$$

where

$$p_i = \begin{cases} 1 - n^{-1}[1 + \xi_i(z_m - u_i)/\sigma_i]^{-1/\xi_i} & \text{if } [1 + \xi_i(z_m - u_i)/\sigma_i] > 0 \\ 1 & \text{otherwise} \end{cases}$$

and (μ_i, σ_i, ξ_i) are the detailed parameters of the point process model for observation i. By taking logarithms of Eq (35),

$$\log\left(1 - 1/m\right) \approx \sum_{i=1}^{n} log(p_i) \tag{36}$$

which combined with p_i as above, we can solve for z_m. Appendix C gives the procedure for obtaining z_m in our chosen model 4 with $m = 5.1591$, which is the observation period (in years) between last crisis until now (Week 15, 2003- Week 25, 2008). The procedures actually solve the equation system with unit roots

method, which is deterministic.

The returned value is obtained as

$$z_m = -0.4143$$

given the estimated series of (μ_i, σ_i, ξ_i) in Model 4. This z_m indicates that the return level of 5.16 years of observation is approximately -0.4143. It's close to the maxima of log-rho ratio series recorded as -0.6895, which took place 2 weeks before the snow began to melt in 2003. In the same way (by adjusting the m in Appendix D), we can have the z_m for $m = 10$ as 0.0086. The extreme power situation in the winter of 2002 is more plausible than the previous analysis had claimed. That is, the abrupt scenarios of the power situation with the same magnitude as the one in winter 2002/3 has a higher frequency than once per 10 years, based on the result of simulation. Even though hydrologists asserted that the rare events like 2002/3 recur only every 100-200 years, when taking into account the stochastic demand and inflow jointly, it still calls for our attention with regard to the reliability of supply.

m	Z_m	95% CI
5.16	-0.4143	[-0.4241, -0.3616]
10	0.0086	[-0.0047, 0.0285]
20	0.4782	[0.4129, 0.4840]
50	1.2518	[1.2402, 1.2618]

Table 2: Different return level estimation with the confidence interval given by section 5.4.2. Confidence intervals are approximated by simulation.

5.4.2 Estimation of confidence intervals by simulation

So far, what we have obtained about the return levels does not include the uncertainty. The estimation of standard errors or confidence intervals for return

levels is realized by a crude approximation based on simulation. Since the sampling distribution of $\theta = (\mu, \sigma, \xi)$ is unknown, we simulate the distribution of θ with multivariate normal approximation. If we denote the maximum likelihood estimate by $\hat{\theta}$, it approximately follows multivariate normal distribution

$$\hat{\theta} \sim N(\theta, V) \tag{37}$$

where V is the estimated variance-covariance matrix from Model 4. We simulate from this distribution k times to obtain $\theta_1^*, \cdots, \theta_k^*$, which constitute a sample from the approximate sampling distribution of the maximum likelihood estimator. For each θ_j^*, substituted into (36), we can solve for $z_{m,j}$. It's a realization from the approximate sampling distribution of $\hat{z_m}$. In the simulation in Appendix D, let $k = 300$, **R** gives a distribution of approximated z_m when $m = 5.16$. The simulated return levels z_m are given as the following Figure 11. And the relative positions of the estimated z_m and their approximations are given in Figure 12. We can judge from the simulated densities that the estimated z_m lie within the approximated intervals.

we can see from above that the estimated value lies within the upper and lower bounds of a 95% confidence interval, which turns out to be $[-0.4241, -0.3616]$. The same analysis applies to the case of $z_m = 10,\ 20,\ 50$. There is also positive bias in the estimation of z_m, i.e. the estimated z_m are relatively smaller than the simulated ones.

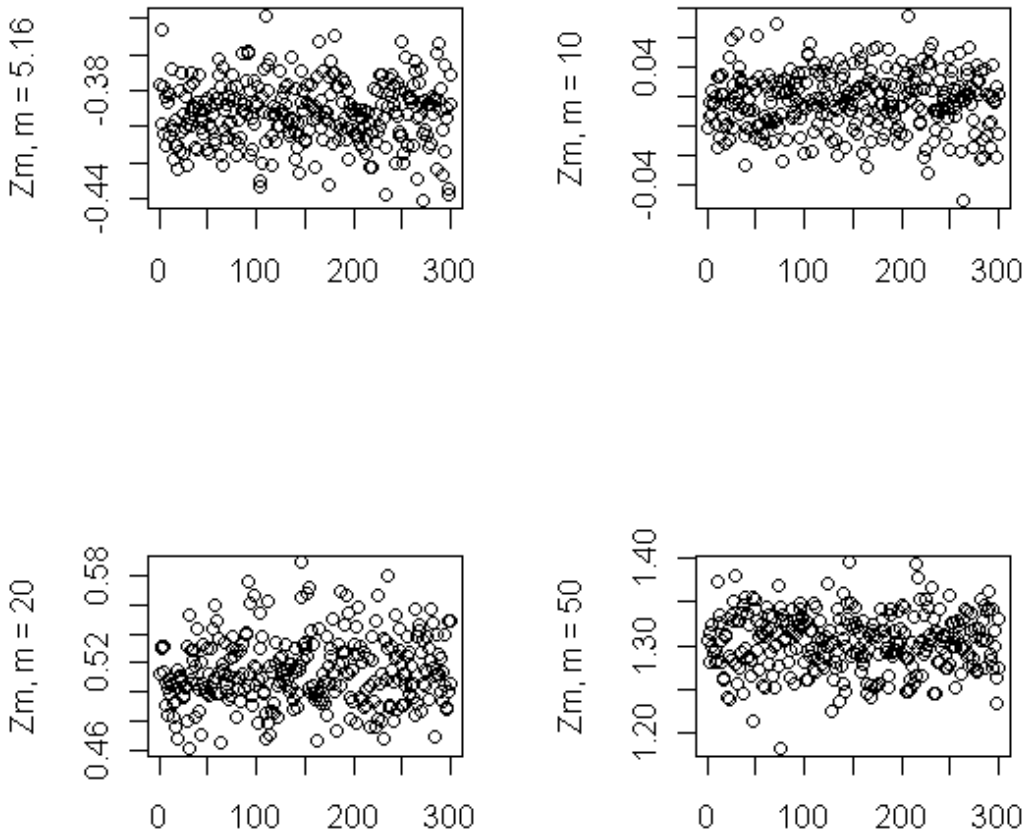

Figure 11: To give the return levels an approximation, we simulate 300 times of Zm.

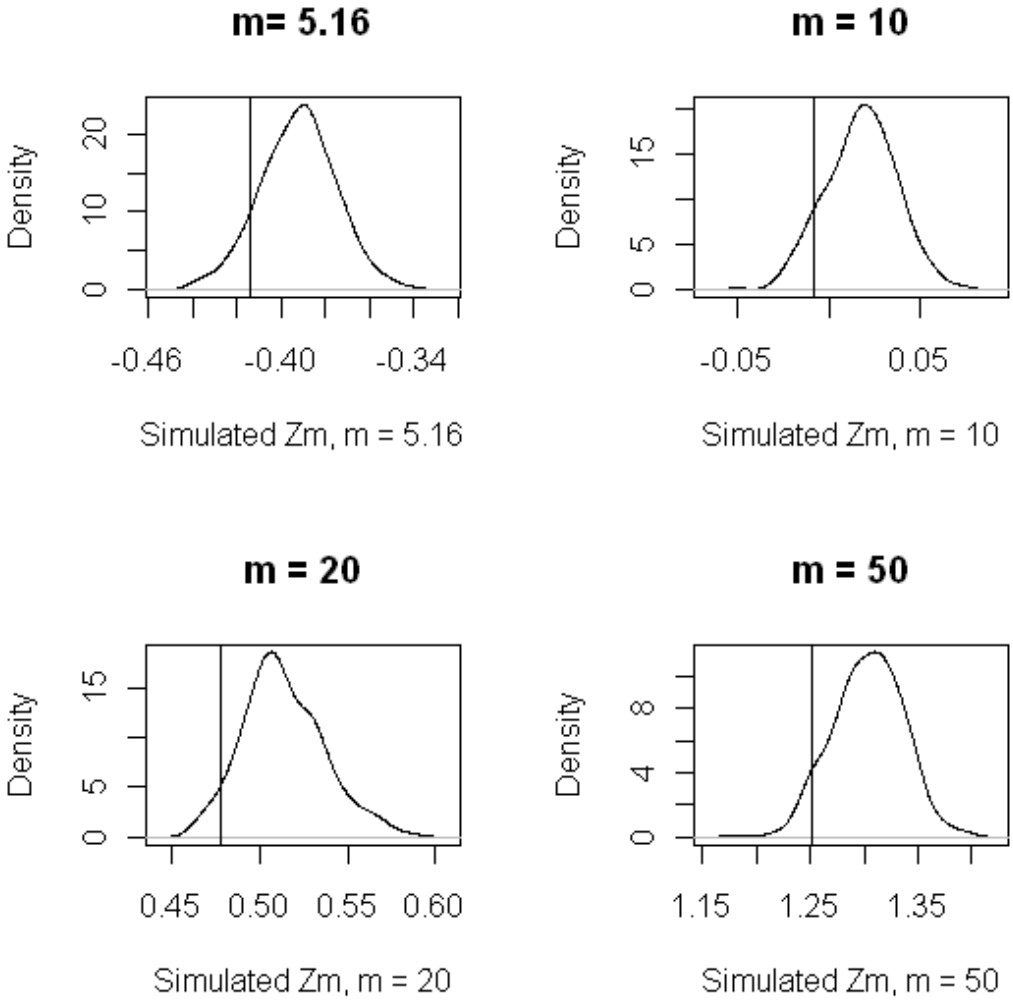

Figure 12: Simulated Densities of return levels, where the estimated z_m lie within the approximated intervals.

6 Conclusion and remark for the further research

This thesis tries to fill the void of analyzing the extreme behavior of power situation on both the supply and demand sides simultaneously, which hasn't been properly done in the literature as far as I know.

The model indicates that severe market shocks in terms of price increases and production - consumption adjustments are likely to occur in the future in a deregulated power regime, as in this thesis, Norwegian power market. And the probability of returning to a level as in year 2002/3 is pretty high. In another word, given the adjustment of the deregulated market system, the power situation as in the winter of 2002/3 would return at a frequency of once per less than 10 years. This result, once refined by a more comprehensive data set, can provide a better understanding of the Norwegian power security. It might be helpful to the decision makers in the government, since it estimates the probability of having a crisis, of given degree of severity, assuming the government keeps the market mechanism unchanged. I find that the Nordic electricity market needs generation investments and more interconnections to other forms of energy form, such as thermal systems, to avoid a crisis such as that in the winter 2002/3 with intervals as low as some 10 years. This rather alarming finding is in contrast to what Amundsen and Bergman (2007) found when only investing the supply side (see the citation in section 1.1.

This conclusion agree with the qualitative analysis of Glende et al (2005). They claimed that the present (as early as in 2005) interconnections are insufficient to handle the huge Norwegian hydrological variations between wet and dry years. This is why Statnett (the system operator assigned by the Norwegian White Paper on Security of Supply) for many years has spent a lot of efforts to establish HVDC connections to other markets. The latest project is NorNed between Norway and the Netherlands.

In a liberalized market there are no mandatory expansion plans that determine which generation units have to be installed in the system and when. Instead,

market participants decide on their own, according to their business expectations, whether they want to build a certain facility or not. This is the reason for the regulators' concern about whether there will be enough installed capacity to meet demand in the long term. To leave everything into the hand of markets or to influence the market by intervention is a problem confronted by each regulatory entity.

There are still some problems and the potential improvements in the analysis in previous sections:

1. Data limitation hampers the inference of the model in this thesis, i.e. the standard errors in the estimation could be lower in the presence of the daily data set for inflows and reservoir levels, if they are available. By feeding data with higher frequency, for instance, daily rho-ratio data into the model, the variance in inference is expected to be considerably reduced and quality-of-fit of the periodic model would be reasonably improved. And the threshold can be chosen in a much easier and reasonable way. But in this thesis, there are only 85 exceedances left in the estimation. Provided with more data, the results from models can be more robust and credible.

2. Using the bivariate extreme value distributions (Tawn, J.A., 1988) to analyze both the demand and supply sides of electricity market altogether, instead of using univariate models as in this thesis might be a nice choice in the future research. Because in our problem setting, there is a need for models of dependence between extremes from different sources: one is from the temperature or other factors of the demand side, the other is the supply side, which is mainly determined by precipitation. Both processes have their own distributions. Introducing the rho-ratio can to some extent simplify the analysis. But the information in 2 different series may well be depressed. Some parametric models have been developed to give a dependence structure between 2 underlying processes. (J. A. Tawn, 1988)

3. The issue of energy securities and their solutions should have been treated by a quantitative approach, as proposed in this thesis. Even though to a

large extent, the case in Norway is unique, the method proposed in this thesis can still be extended to other forms of renewable energy, such as wind power, which is the part of the portfolios of many countries at present. As can been seen in many models, the Weibull model closely mirrors the actual distribution of hourly wind speeds at many locations. With the GEV distribution readily available, the extreme behavior of the production volume of wind farms can be easily obtained.

Reference

Adib,P., Schubert,E. and Oren,S. (2008). Resource Adequacy: alternate perspectives and divergent paths, *Competitive Electricity Markets: Design, Implication, Performance* ,chapter 9, 327-362.

Amundsen,E.S. and Bergman, L.(2007). Integration of multiple national markets for electricity: The case of Norway and Sweden, *Energy Policy* 35(6)3383-3394.

Borenstein, S. (2000). Understanding Competitive Pricing and Market Power in Wholesale Electricity Markets, *The Electricity Journal*, Volume 13, Issue 6, 3 July 2000, Pages 49-57.

Bye,T. , Bruvoll, A. and Aune, F.R.(2008). Inflow shortages in deregulated power markets- reasons for concern?, *Energy Economics*, 30:1693-1711.

Coles, Stuart.(2001). An Introduction to Statistical Modeling of Extreme Values, *Springer series in Statistics*, Springer.

Crampes, C. and Moreaux, M. (2001). Water resource and power generation, *International Journal of Industrial Organization*, 19:975¨C99.

David,A.K. and Wen, F. (2001). Market power in electricity supply, *IEEE Transcations on energy conversion*, Vol.16, No.4 Dec 2001.

Embrechts, P. Kluppelberg, C. and Mikosch, T. Modeling Extremal Events: for Insurance and Finance. (1997). Series: Stochastic Modeling and Applied Probability , Vol. 33. ISBN: 978-3-540-60931-5.

Fleten, S.E., Wallace, S.W, Ziemba, W.T.(1997) Portfolio management in a deregulated hydro power based electricity market,1997, *Proceedings Hydropower* Norway, July.

Fosso, O.B., Gjelsvik,A., Haugstad,A. Mo,B. Wangensteen, I.(1999). Generation scheduling in a deregulated system. The Norwegian case, *IEEE Transactions on Power Systems*, vol **14**, Feb (1999).

Glende,I. Tellefsen,T. and Walther, B. (2005). Norwegian System Operation facing a Tight Capacity Balance and Severe Supply Conditions in Dry Years, *Hydropower'05*, Stavanger Norway, 23-25 May 2005.

Hanssen, B.I., Forland, E.J., Haugen, J.E., Tveito, O.E. (2003). Temperature and precipitation scenarios for Norway: comparison of results from dynamical and empirical downscaling. *Climate Research* 25:15-27.

Johnsen, T.A., Verma, S.K. and Wolfram, C. (1999) Zonal pricing and demand-side bidding in the Norwegian electricity market, Working Paper, *Program on Workable Energy Regulation (POWER)*, June.

Johnsen, T.A. (2001). Demand, generation and price in the Norwegian market for electric power, *Energy Economics* 23: 227-251.

Laukkanen, A. (2004). Handling of special days in demand forecasting model for Nordic power market, Helsinki University of Technology, *Systems analysis laboratory.*

Smith, R.L. (1989). Extreme Value Analysis of Environmental Time Series: An Application to Trend Detection in Ground-Level Ozone, *Statistical Science*, Vol. 4, No. 4, (Nov., 1989), pp. 367-377.

Tawn, J. A. (1988). Bivariate extreme value theory: Models and estimation, *Biometrika*, 75(3):pp.397-415.

Vehvilainen, I. and Pyykkonen, T. (2005). Stochastic factor model for electricity spot price- the case of the Nordic market, *Energy Economics* 27 (2) 351-367.

Visudhiphan,P. and Ilic, M.D. (2000). Dependence of Generation Market Power on the Demand/Supply Ratio: Analysis and Modeling, *2000 IEEE*, 1115-1122.

Vries, L.J. and Hakvoort, R.A. The Question of Generation Adequacy in Liberalised Electricity Markets, *The Fondazione Eni Enrico Mattei Note di Lavoro Series* Index: http://www.feem.it/Feem/Pub/Publications/WPapers/default.htm.

Appendix

A Data Masking

The raw data are *weekdemand*, *weekproduction*, *reservoir* and *capacity*. They are expected to be saved as *.txt* files under the assigned **R** dir. The following procedures read the data into workspace and computes the $inflow$ and rho as needed. There is one period of gap between the ordered data points in the vector of inflow and reservoir.

```
#Read in the data from assigned dir
weekdemand<- scan("weekdemand 381.txt")
# week 9,2001  - week 24,2008/381
weekproduction<- scan("weekproduction 381.txt")
#  week 9,2001  - week 24,2008/381

# Inflow at period t
reservoir<- scan("Reservoir 383.txt")
# week 9,2001 - week 26,2008/383
capacity<- scan("capacity 383.txt")
# week 9,2001  - week 26,2008/383
res.delta<-reservoir[3:383]- reservoir[2:382]
length(res.delta)
# gap  week 9,2001  - week 24,2008/381
res.minus<- reservoir - capacity*.15
#   week 9,2001  - week 26,2008/383
length(res.minus)

inflow<- weekproduction + res.delta
# week 9, 2001- week 24,2008/381
length(inflow)
cont.infl<- inflow+ res.minus[1:381]

#  week 9, 2001  - week 24,2008/381
length(cont.infl)

# Calculating log-rho ratio
logrho<- log(weekdemand*0.001)-log(cont.infl)
# week 9, 2001- week 24,2008/381
```

B Point Process fitting with R

The procedures of fitting Model 1 to 7 are as follows. Five different models can be fitted by varying reverse link function and covariates, which is summerized by the following table

Model	**mul**	**mulink**	**sigl**	**siglink**	**shl**	**shlink**
1	-	-	-	-	-	-
2	2	identity	-	-	-	-
3	2	identity	2	exp	-	-
4	2	identity	2	exp	2	identity
5	1:2	identity	2	exp	2	identity
6	1:2	identity	1:2	exp	2	identity
7	1:2	identity	1:2	exp	1:2	identity

Table 3: Parameter settings in 7 different models.

This table corresponds to Table 1. It further specifies the settings in the $fpp(\cdot)$, which is a function of *extRemes* package allows for the covariates in each of the parameters. Function $fpp(\cdot)$ consists of 10 key parameters.

> fpp(xdat, threshold, npy = 365, ydat , mul , sigl, shl, mulink, siglink, shlink)

Assigning different values to the parameters yields different model settings. This is realized by setting *mul*, *sigl* and *shl*. For example, letting $mul = 2$ allows the periodity in location parameter μ and letting $mul = 1 : 2$ means there is not only periodity but also the linear trending in μ. The *inversed link function* could be exponential in the case of σ (in order to preserve the positivity of σ) and identity in the case of μ. Different models take the form of different combinations in settings of 3 parameters.

Before running the estimation, the package *extReme* has to be in place. The main steps are

- Setting up time-varying threshold by trial-and-error.
- Define the covariates *ydat* in a form of 381 by 2 matrix.

- Defining the parameters in function $fpp(\cdot)$. Such as the npy, which is equal to 52.14 since we are using the weekly data.
- Runs the MLE in **R**.
- **R** returns the estimated parameters and other relevant values if any (SE, $nllh$, $conv$ and $nexc$, etc.) The result of our model is summerized in Table 1.

The procedures and returned results are as follows:

```
> # Setting up time-varying threshold by trial-and-error
> t<- matrix(1:381,nrow=381);
> u<- -2.6+0.81*cos(2*pi*t/52.14-.18);
> plot(rho, xlab= "Week Index", ylab="rho and u "); lines(u)

> # Define the covariates, which is a (381 x 2) matrix
> y<- cbind(t, cos(2*pi*t/52.14-.18));

> # Fit the rho process into the Point Process model

> # Model1, homogenous case
> model1<- fpp(rho, u, npy=52.14, ydat=y)

$model

$model[[1]]
NULL

$model[[2]]
NULL

$model[[3]]
NULL


$link
[1] "c(identity, identity, identity)"

$npy
[1] 52.14
```

```
$nexc
[1] 85

$conv
[1] 0

$nllh
[1] -123.4567

$mle
[1] -1.2818986  0.8326420  0.2009234

$se
[1] 0.2769358 0.2594025 0.1374783

##############################

> # Model2, periodic in 'mu'
> model2<- fpp(rho, u, npy=52.14, ydat=y, mul=2, mulink=identity)
$model
$model[[1]]
[1] 2

$model[[2]]
NULL

$model[[3]]
NULL


$link
[1] "c(identity, identity, identity)"

$npy
[1] 52.14

$nexc
[1] 85

$conv
[1] 0

$nllh
```

```
[1] -180.7753

$mle
[1] -2.0663095  0.7596313  0.2686604  0.2082541

$se
[1] 1.999819e-06 1.999819e-06 1.999819e-06 1.999819e-06

##############################

> # Model3, periodic in 'mu' and 'sigma'#
> model3<- fpp(rho, u, npy=52.14, ydat=y, mul=2, sigl=2, mulink=identity,
+ siglink= exp)
$model
$model[[1]]
[1] 2

$model[[2]]
[1] 2

$model[[3]]
NULL


$link
[1] "c(identity, exp, identity)"

$npy
[1] 52.14

$nexc
[1] 85

$conv
[1] 0

$nllh
[1] -183.5229

$mle
[1] -2.09884332  0.92759914 -1.63239043  0.40024856 -0.00956952

$se
```

```
[1] 0.05803717 0.06825643 0.22653570 0.17073094 0.14425005

##############################

> # Model4, periodic in 'mu', 'sigma' and 'xi'#
> model4<- fpp(rho, u, npy=52.14, ydat=y, mul=2, sigl=2, shl=2,
 mulink=identity, siglink= exp, shlink=identity)
$model
$model[[1]]
[1] 2

$model[[2]]
[1] 2

$model[[3]]
[1] 2


$link
[1] "c(identity, exp, identity)"

$npy
[1] 52.14

$nexc
[1] 85

$conv
[1] 0

$nllh
[1] -185.6654

$mle
[1] -2.1850185  0.9286292 -2.0059722  0.9347711 -0.1117706  0.3763738

$se
[1] 0.04608098 0.04794619 0.10436186 0.07943438 0.04339337 0.04339337


##############################

> # Model5, periodic in 'mu', 'sigma' and 'xi'; also with linear trend
```

```
 in 'mu' and 'sigma'#
> model5<- fpp(rho, u, npy=52.14, ydat=y, mul=1:2, sigl= 2, shl=2,
 mulink=identity, siglink= exp, shlink=identity)
$model
$model[[1]]
[1] 1 2

$model[[2]]
[1] 2

$model[[3]]
[1] 2


$link
[1] "c(identity, exp, identity)"

$npy
[1] 52.14

$nexc
[1] 85

$conv
[1] 0

$nllh
[1] -183.8906

$mle
[1] -2.080167e+00 -9.966421e-05  9.104215e-01 -1.450991e+00  4.164851e-01
[6]  1.624703e-01  9.543880e-02

$se
[1] 1.999816e-06 1.999711e-06 1.999816e-06 1.999816e-06 1.999816e-06
[6] 1.999816e-06 1.999816e-06

##############################

> # Model6, periodic in 'mu', 'sigma' and 'xi'; also with linear trend
 in 'mu' and 'sigma'#
> model6<- fpp(rho, u, npy=52.14, ydat=y, mul=1:2, sigl=1:2, shl=2,
 mulink=identity, siglink= exp, shlink=identity)
```

```
$model
$model[[1]]
[1] 1 2

$model[[2]]
[1] 1 2

$model[[3]]
[1] 2


$link
[1] "c(identity, exp, identity)"

$npy
[1] 52.14

$nexc
[1] 85

$conv
[1] 10

Warning message:
In sqrt(diag(z$cov)) : NaNs produced
> pp.diag(model6)
>
> # Model7, periodic in 'mu', 'sigma' and 'xi'; also with linear trend
 in 'mu' and 'sigma'#
> model7<- fpp(rho, u, npy=52.14, ydat=y, mul=1:2, sigl=1:2, shl=1:2,
 mulink=identity, siglink= exp, shlink=identity)
Error in optim(init, pp.lik, hessian = TRUE, method = method, control =
 list(maxit = maxit,  :
  non-finite finite-difference value [1]
> pp.diag(model7)
Error in pp.diag(model7) : object "model7" not found
```

C Procedures for obtaining return level z_m by solving a non-linear equation system

The system of non-linear equations given by p_i and (36) is solved by using *uniroot*( ) in **R**. We first define a function of z_m and then obtain the uniroot of $f(10) = 0$ by:

```
# Calculate the return level from Model 4
# Redefine the parameters w.r.t. Model 4
miu<- model4$vals[,1]
sigma <- model4$vals[,2]
xi<- model4$vals[,3]

# Define the f(.) function
f<-function(zm) I%*% log(1-pmax(1+xi*(matrix(zm, nrow=N)-miu)/sigma,
 matrix(0,nrow=N))^(-1/xi)/52.14)-log(1-1/m)

uniroot(f, c(-1,2),lower=-1, upper=2,
f.lower=f(-1),f.upper=f(2),tol=0.00001)
```

and the z_m with $m = 10$ is returned as

```
$root
[1] -0.008472016

$f.root
             [,1]
[1,] 3.653591e-07

$iter
[1] 9

$estim.prec
[1] 5e-06
```

In the same way, we could have the return levels for $m = 5.159187, 30, 50, 100$ etc.

D Confidence interval of Return Level z_m

We use the function $rmnorm(\cdot)$ in package $mnormt$ to simulate the 381 by 3 parameter matrix θ for $k = 300$ times by following scripts:

```
> # Simulation for the approximate sample distribution of theta
> # Define the times of simulation
> N<- 381
> # Define the f(.) function. m is set to 5.16 years
> m<- 5.159187
> I<- matrix(1, ncol= N)
> f<-function(zm) I%*% log(1-pmax(1+xi*(matrix(zm,
 nrow=N)-miu)/sigma,matrix(0,nrow=N))^(-1/xi)/52.14)-log(1-1/m)
>
> #zm is first defined to be an empty vector
> zm = matrix(0,nrow= 300);
>
> for (count in 1:length(zm)){
# Random sampling in Multivariate normal approximation
+ sampling<- rmnorm( n= N, mean = model4$mle, varcov= model4$cov);

# Redefine the "miu", "sigma","xi" in functin f(.)
# through linking function h(.)
+  miu<- sampling[,1]+ sampling[,2]* y[,2];
+  sigma <- exp(sampling[,3]+ sampling[,4]* y[,2]);
+  xi<- sampling[,5]+ sampling[,6]* y[,2];

+ # Solve the return level 'zm' with m-years
+ zm[count,1]<-uniroot(f, c(-1,2),lower=-1, upper= 2,
 f.lower=f(-1), f.upper=f(2), tol=0.0000001)$root;
+ }
```

R returns the approximate sampling distribution of z_m. In this case, m is set to be 5.16 years, which is equivalent to the observation period between Week 15, 2001 and Week 25, 2008.